REVIEW PAPER

Microactuators technologies for biomedical applications

Mariatul Rawdhah Ahmad Fuaad[1] · Mohammed Nazibul Hasan[2] · Muhammad Izzudin Ahmad Asri[1] ·
Mohamed Sultan Mohamed Ali[1]

Abstract

Rapid advancements in technology have facilitated the development of functional micro-electromechanical system (MEMS) actuators. The use of such actuators has recently witnessed a surge in a variety of biomedical applications, owing to their high precision and conformity. This review aims to provide a comprehensive survey of the recently developed MEMS actuators and their use in biomedical applications. In the context of these applications, we discuss the most appropriate and extensively used actuation techniques such as thermo-responsive, magnetic, piezoelectric, and soft actuation. In addition, state-of-the-art biomedical systems, tools, and devices are categorically reviewed with recently utilized actuation techniques, to provide insight into the prospects of implementation. The key parameters responsible for the enhanced performance and efficiency of the actuators were also addressed. Finally, the future research trends in actuation techniques for biomedical applications are discussed.

1 Introduction

In recent years, soft actuators for medical devices have seen an increase in popularity in terms of research and production. The development of conventional actuators as assistive tools has significantly aided in risk minimization during medical procedures. Therefore, it is important to offer precise surgical procedures with high accuracy, durability, and safety. Therefore, dedicated actuation mechanisms are required. With advancements in technology, micro-electromechanical system (MEMS) technology-based actuators are becoming increasingly useful for improving the precision and regulation of movement and versatility in a variety of medical systems, instruments, and devices. MEMS-based actuators convert specific energy domains into mechanical movements on a microscopic scale. Such tools enable us to explore the human body through tortuous trajectories while minimizing the risk of tissue damage and exhibiting a low interaction force with organs. The integration of actuators into endoscopic medical devices can help control the movements of equipment used in treatment, in addition reducing the likelihood of human error (Takizawa et al. 2018; Wang et al. 2020; Perez-Guagnelli et al. 2020). The advantageous characteristics of actuation mechanisms in these devices lead to numerous benefits for both patients and medical service providers, such as shortened treatment times, reduced post-surgery effects and patient discomfort (Beasley et al. 2012). Therefore, it is crucial to develop appropriate actuation mechanisms to drive specific tasks in medical devices.

The capabilities of MEMS actuators are continuously growing as they demonstrate significant potential for various applications. However, each MEMS actuator has its own set of characteristics and limitations. Among the existing MEMS actuators, thermo-responsive, electromagnetic, piezoelectric, and soft actuation techniques possess appealing features and have been widely used in a variety of biomedical devices. Shape memory polymers (SMPs) and shape memory alloys (SMAs) are smart materials that respond to thermal stimuli. SMPs offer high elastic deformation, structural flexibility, and large strains, (Zainal et al. 2017) whereas SMAs provide high work density, large actuation force, simple structural design, and biocompatibility (Zainal et al. 2015; AbuZaiter and Ali 2014; Abu-Zaiter et al. 2015a). Alternatively, piezoelectric actuators are often used in high-speed and high-precision applications owing to their characteristics of high accuracy, large-stroke, lightweight, and fast response (Wang et al. 2019;

✉ Mohamed Sultan Mohamed Ali
sultan_ali@fke.utm.my

1   Faculty of Electrical Engineering, Universiti Teknologi Malaysia, UTM Johor Bahru, 81310 Johor, Malaysia

2   Division of Solid-State Electronics, Department of Electrical Engineering, Uppsala University, SE-751 03 Uppsala, Sweden

Shi et al. 2013; Ding et al. 2019; Li et al. 2015; Jain et al. 2015). Whereas, electromagnetic actuators typically provide a large displacement, simple drive mode, high field energy density, remote control achievable with low input voltages, and rapid dynamic response (Lee et al. 2009; Kim et al. 2005). Finally, soft actuators are mainly used in medical applications that require high flexibility. For instance, pneumatic actuators are popular as they are well known for their low production costs, simple structure, high flexibility, high force per unit volume, and high energy density (Rehman et al. 2017; Paez et al. 2016; Sonar et al. 2020; Rehman et al. 2019). In addition to these actuation techniques, new emerging soft actuation technologies, including ionic-polymer metal composite (IPMC), dielectric elastomer (DE), and hydraulically amplified self-healing electrostatic (HASEL), have exhibited high potential for use in biomedical devices.

Considering the potential of MEMS actuators, several studies on soft actuation have been conducted, with an emphasis on their recent applications. For instance, Ghazali et al. (2020) studied MEMS actuators developed for biomedical applications and their key applications. Other researchers have focused on specific types of actuations, such as electromagnetic (Yunas et al. 2020), piezoelectric (Salim et al. 2018), thermo-responsive (Ariano et al. 2015), and soft actuation (Mohith et al. 2019; Bar-Cohen et al. 2019; Hao et al. 2019). However, prior discussion demonstrated a limited scope, as subjects on soft actuators were rarely covered in-depth, despite being an appealing feature for the biomedical field. Sénac et al. (2019) and Gifari et al. (2019) reviewed surgical and endoscopic devices, while Tetteh et al. (2014) and Munoz et al. (2014) focused on drug delivery systems. Nevertheless, these studies have mostly focused on specific biomedical applications.

In contrast, the current review emphasizes four primary MEMS actuation methods: thermo-responsive, electromagnetic, piezoelectric, and soft actuation, and their application in biomedical areas including drug delivery systems, medical tools, and artificial muscle. In addition, this study discusses the newly discovered HASEL actuators and their potential for biomedical applications. The actuator mechanism, configuration, fabrication, and performance are extensively discussed. Furthermore, this study classifies each type of actuation of the actuators deployed for various biomedical applications. A graphical description of the review is presented in Fig. 1. The remainder of this paper is organized as follows. The working principle and essential features of the actuators are discussed in Sect. 2. Section 3 presents the key applications of actuators in medical devices in terms of their actuation mechanisms, tools, and devices, along with a comparison of their output performance. Finally, the review concludes with a synopsis of the main outcomes, implications, and future prospects of these actuators in Sect. 4.

2 Types of actuations

This section focuses primarily on MEMS actuators, including thermo-responsive, magnetic, piezoelectric, and soft actuation techniques. Their working mechanisms and features are also discussed.

2.1 Thermo-responsive actuation

Thermo-responsive actuation is a type of actuation that enables thermo-responsive materials to change their physical structure in response to a thermal stimulus. SMA and SMP are thermo-responsive materials that respond to heat; they are widely used in biomedical devices. Both SMA and SMP actuators are discussed in this subsection.

2.1.1 SMA actuator

SMA is a class of metallic materials that have the ability to restore a previously specified length or shape when subjected to a thermodynamic process. SMAs are actuated by the shape memory effect (SME), also known as the monoclinic crystal form (martensitic) and the cubic crystal form (austenitic) transformation. The austenite phase is stable at high temperatures, while the martensite phase is stable at low temperatures. The transitions in the crystalline state of SMA are depicted in Fig. 2a. When SMA is in its martensite phase, the alloy is composed of monoclinic crystals, rendering it more flexible and thus more easily deformed. When heated above the austenite temperature, cubic crystals are formed within the molecular arrangement, causing the material to become rigid and difficult to deform (AbuZaiter et al. 2015b; Han et al. 2016). When the SMA is cooled without a load, the crystal structure of the material resembles that of twinned martensite. During this phase, the SMA can be deformed by applying an external force or employing a bias spring to achieve reversible motion.

SMA actuation modes include one-way and two-way actuation, as shown in Fig. 2b. The SMA returns to its original shape at the austenite phase temperature in one-way actuation mode, but an external force is needed to recover its deformed shape. While in two-way actuation mode, the SMA is conditioned to remember its form in both the austenite and martensite phases by undergoing a training process. However, achieving a two-way actuation mode is a lengthy process due to the repeated heating training process, prompting researchers to investigate different methods of achieving two-way actuation using bilayer actuation (Ren et al. 2020). Bilayer actuation occurs when two thin materials with different coefficients of thermal expansion are kinematically constrained together.
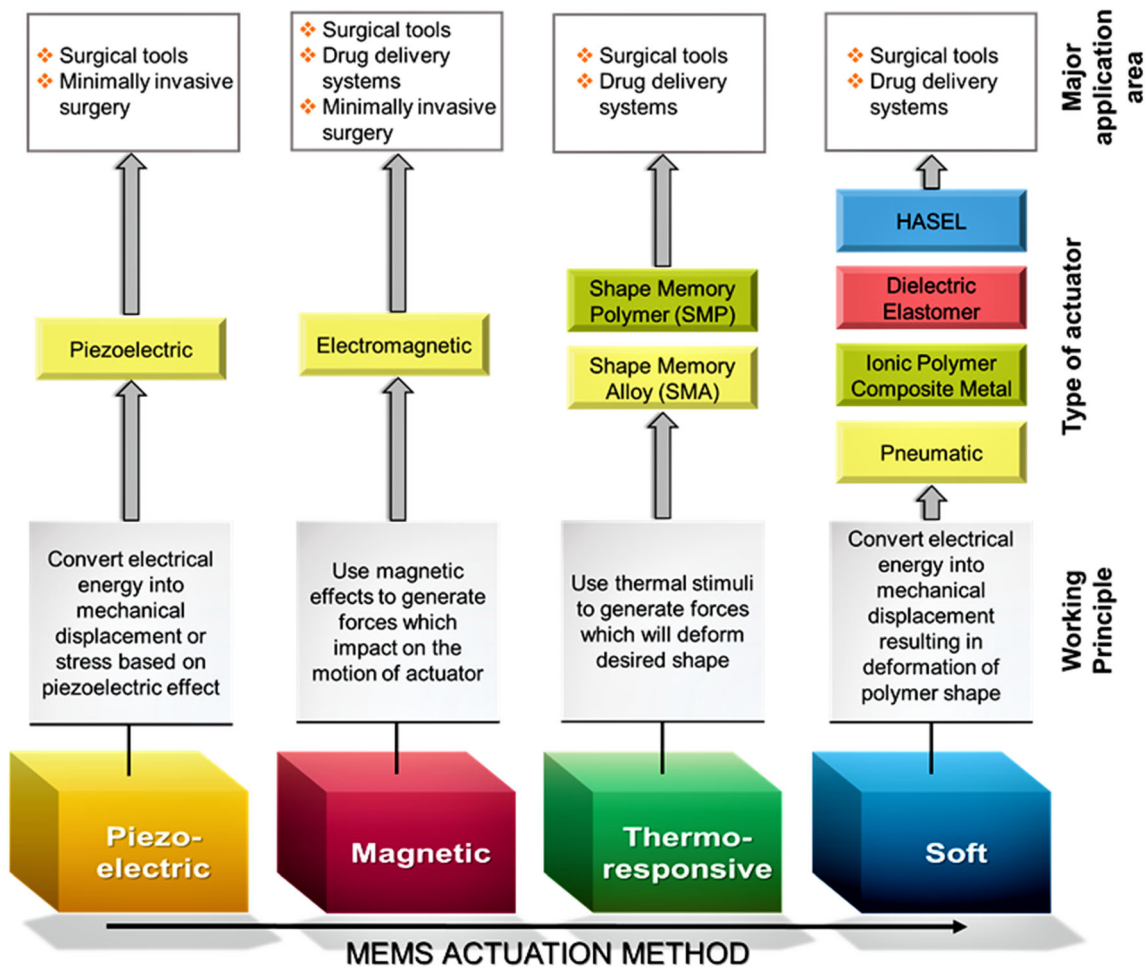
Fig. 1 Graphical overview of the paper on MEMS actuation techniques

As the temperature changes for two thin materials, different strains in the materials cause the entire structure to bend. For instance, AbuZaiter et al. (2016a, b) and Ali et al. (2012) developed a bimorph SMA structure with silicon dioxide (SiO_2) that provides a maximum displacement of 804 µm and an out-of-plane displacement of 466 µm. In addition, Kabla et al. (2016) presented a novel concept for in-plane actuators based on a thin free-standing SMA film connected with a spring made of four silicone folded beams.

SMAs are composed of a few elements that determine their transformation temperature. Among the various SMA families (e.g., TiNiCu, CuAlNi, NiAl), NiTi-based alloy has been widely used in biomedical applications due to its biocompatibility property (Thierry et al. 2002) and its superelastic behavior (Shabalovskaya 1996). They are usually composed of patterned thin film or bulk-micromachined structures (Choudhary and Kaur 2016; Jayachandran et al. 2019). SMA actuators have appealing characteristics such as high displacement, large force, high mechanical robustness, large work density, and good resistance to corrosion (AbuZaiter and Ali 2014; AbuZaiter et al. 2015a; Munasinghe et al. 2016; Sassa et al. 2012; Zainal et al. 2015). For instance, AbuZaiter et al. (2016a, b) has created a micromanipulator with a gripping mechanism powered by an SMA bimorph actuator. The designed micromanipulator achieves high displacement and a substantial degree of freedom. However, the general drawbacks of SMA actuators include their relatively slow temporal response and high power consumption when actuated with self-heating by passing an electrical current through the material (Holman et al. 2021; Mehrpouya and Cheraghi Bidsorkhi 2016).

2.1.2 SMP actuator

Akin to SMAs, thermo-responsive SMPs have also garnered the interest of researchers for their use in biomedical applications including surgical devices, artificial muscle, and drug delivery systems. The characteristics of tailorable transition temperatures, ease of activation, large shape deformation, and recovery time has made thermo-

Fig. 2 **a** SMA crystalline orientation. **b** SMA actuation mode
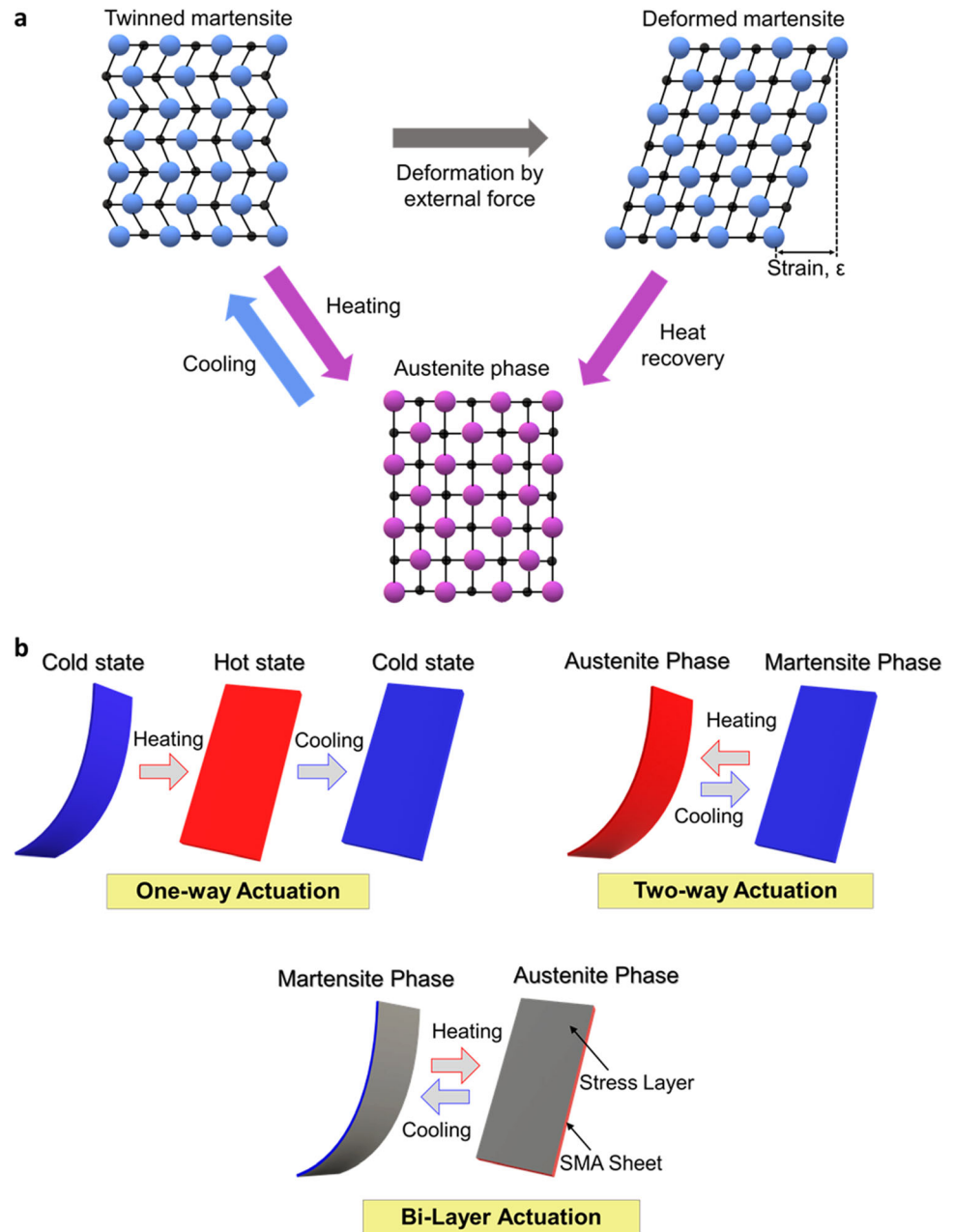
responsive SMPs a great contender for biomedical devices (Sun et al. 2020). The SMP falls under the category of active deformable materials that can be conditioned to remember a temporary shape and return to its original shape in response to thermal stimuli. Like SMA, thermo-responsive SMP also exhibits SME, a remarkable phenomenon of mechanical process embodied by the shape memory cycle. The shape memory cycle in SMP consists of hot and cold phases (Fig. 3a). The first stage is the programming process, in which external force is applied to set the desired shape and an annealing process is conducted. The material is then be cooled to below the transition temperature during the recovery process. At this

stage, the material can be deformed to a temporary shape, and the trained shape can be recovered by heating the material (Fig. 3a).

As illustrated in Fig. 3b, the molecular mechanics of the SME concept is based on the two-phase structure of the polymer, i.e., cross-links and switching segments (Hasan et al. 2016; Mu et al. 2018). The permanent shape of the polymer is determined by cross-links, whereas the temporary shape is determined by switching segments and transition temperature. The SMP is stiff when its temperature is below the transition temperature, and it becomes comparatively soft when heated above the transition temperature. For the switching segments to fix the molecular chain's
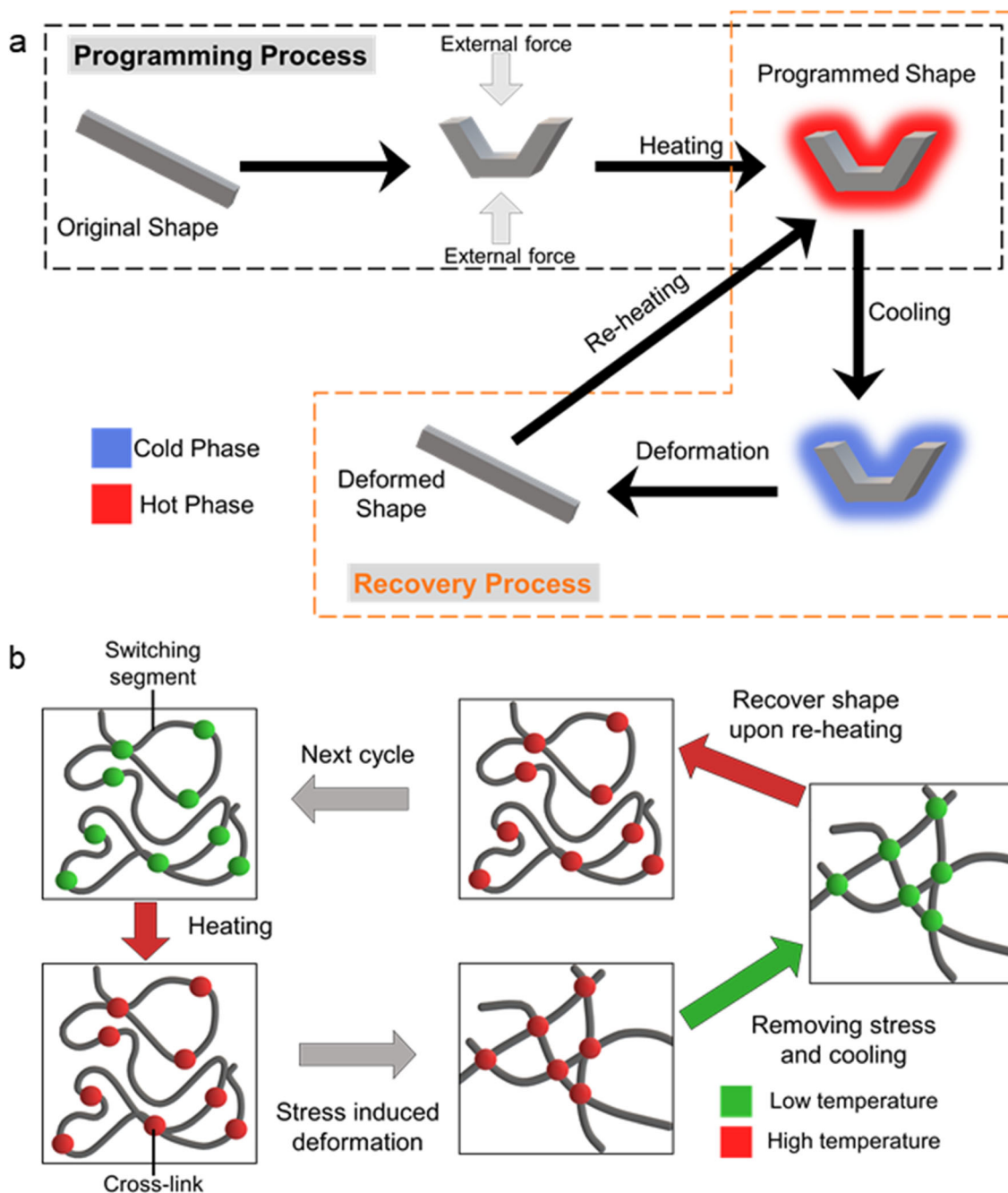
Fig. 3 a Shape memory cycle. **b** Molecular mechanics of SMP

position during shape setting, an external force must be applied to the SMP when heated above the transition temperature. Afterward, the SMP is cooled while the external force is removed, resulting in a polymer with a memorized shape. The shape memory effect is induced when heat is applied to the SMP and the memorized shape is recovered.

The features of SMPs, such as high elastic deformation, remote wireless control, structural flexibility, large strains, and biodegradable properties in some SMPs (Ge et al. 2016; Liu et al. 2007) increase their suitability for use in biomedical devices (Ajili et al. 2009; Wache et al. 2003). For instance, Pringpromsuk et al. (2021) employed shape memory polyurethane and a dibutyl adipate (DBA) plasticizer to create tube actuators that were used as artificial blood vessels. In addition, Zainal and Ali (2016) developed a two-way actuation for an implantable drug delivery system driven and controlled wirelessly by RF magnetic field resonant heating.

Moreover, Besse et al. introduced a concept for reshaping arrays of hundreds of tightly packed flexible SMP actuators by timely synchronizing the thermal stimuli and external pressure, thus allowing each actuator to be controlled independently using low voltage inputs (Besse et al. 2017a, b). Meanwhile, Aksoy et al. (2019) studied and utilized cyclic and latching SMP actuators to produce arrays of individually addressable, latchable, and reversible valves. Despite their numerous advantageous properties, SMPs suffer from the limitations of slow response and low recovery stress. Table 1 shows the performance of the SMA and SMP thermo-responsive actuators that are mainly utilized for applications related to the biomedical field. In terms of displacement, SMA and SMP generally have large displacement output but are heavily dependent on the actuator size. The overall force of SMA shows a higher value compared to SMP, provided that SMA has a large volt-density. In addition, SMA shows a higher frequency value than SMP, but thermo-responsive actuation generally has a slow response. In general, the SMA actuator outperforms the SMP actuator in terms of displacement, frequency, and output force.

2.2 Magnetic actuation

The thermo-responsive actuation methodologies discussed in the previous section mostly require a physical connection to transmit power for the actuation to occur, which leads to higher power consumption and fabrication limitations. In addition, they have slow actuation responses as well as lengthy training processes for SMA and SMP. On the contrary, magnetic actuators provide various benefits, such as higher efficiency and precise structural movement, remote actuation, rapid dynamic response, and manipulation (Kim and Meng 2015). Thus, the concept of magnetically actuated techniques has been researched to improve the number of degrees of freedom (DOFs) while reducing the actuation fabrication and control complexity, and power consumption.

Magnetic actuation can be classified into two types: electromagnetic and magnetostrictive. Electromagnetic actuation necessitates the use of electricity to stimulate magnetic effects. By providing an alternating current to the coil or inductor incorporated into the resonator, it employs the electromagnetic force (Lorentz force) to produce a

Table 1 Performance of thermo-responsive actuators

Type of actuation	Dimension (mm)		Actuation frequency (Hz)	Displacement	Force (N)	DOF	References
	Diameter	Length					
SMA	3.5	60	10	0.7 mm	0.7	2	Namazu et al. (2011)
SMA	0.4	350	NA	1.5 mm	16	6	Yuan et al. (2014)
SMA	0.5	8	0.025	81 mm	NA	2	Kadir et al. (2019)
SMA	100 μm	12	0.08	200 μm	NA	NA	Mehrabi and Aminzahed, (2020)
SMA	NA	20	0.27	95 μm	NA	2	Makino et al. (2001)
SMA	0.4	100	NA	55 mm	7.5	NA	Lu et al. (2019)
SMA	100 μm	10	x: 0.13	8.9 mm	x: 0.11	2	AbuZaiter et al. (2016a, b)
			y: 0.11		y: 0.13		
SMA	4	9	0.05	3 mm	NA	2	Abadie et al. (2009)
SMA	8	250	NA	35 mm	30	3	Shi et al. (2014)
SMA	0.53	101.6	NA	NA	2.5	2	Ayvali and Desai (2012)
SMA	NA	5	20–40	20 μm	5 m	NA	Yanatori et al. (2019)
SMA	NA	1	100	45 μm	115 m	2	Kabla et al. (2016)
SMP	10	NA	153 M	234 μm	NA	NA	Zainal and Ali (2016)
SMP	NA	40	0.03	5 mm	0.073	NA	Zhang et al. (2019a, b, c)
SMP	7	40	NA	NA	0.74	2	Yahara et al. (2019)
M-SMP	15	21	0.017	15 mm	NA	2	Ze et al. (2020)
SMP	1.75	24	NA	10 mm	1.11	2	Yang et al. (2016)
SMP	NA	NA	0.2	650 μm	400 m	NA	Besse et al. (2017a, b)
SMP	3	4	0.03	300 μm	1.5	2	Besse et al. (2017a, b)
SMP	7	9	0.025	10 mm	0.03	2	Chen et al. (2019a, b)
SMP	3	15	0.03	200 μm	NA	1	Aksoy et al. (2019)
SMP	NA	20	0.5	0.18 mm	NA	2	Pringpromsuk et al. (2020)

magnetic field in the resonator. The Lorentz force is the force generated on a point charge by the combined electric and magnetic forces acting on it. When an electric current (i) flows through a conductor, i produced an external magnetic field (B) resulting in a Lorentz force, as stated by (1) (Younis 2011):

$$F = B\text{i} \times \text{L} \tag{1}$$

where L signified the length of the conductor. An electromagnetic force perpendicular to the current and the magnetic field is generated by the current in the conductive element placed within the magnetic field. The applied current to the coil then creates a mechanical displacement due to the interaction generated by the current between the magnet and the magnetic field (Algamili et al. 2021).

Electromagnetic actuation involves the interaction of magnetic structures and B generated by a current-carrying circuit (Yang and Xu 2017). As shown in Fig. 4a, a magnetic actuator comprises of an excitation coil and a ferromagnetic movable structure mounted in the field formed by the coil, with the movable magnetic structure being a suspended cantilever beam (Baù et al. 2008; Bau et al. 2009). When i is passed through the coil, it produces B defined by Biot–Savart law (Gomis-Bellmunt and Campanile 2009; Lv et al. 2015) as:

$$B = \mu_0 \mu_r \frac{N_i}{1} \tag{2}$$

where μ_0, μ_r, N_i, and l are the permeability of free space, the relative permeability of the material, the number of coil turns, and the length of the coil, respectively. The interaction with B induces an attractive force, F, acting on the cantilever beam to cause a displacement, X, (refer to Fig. 4b) at the beam's free end, which can be expressed as (Sheeparamatti and Naik 2016):

Fig. 4 Schematic diagram of the working mechanism of an electromagnetic actuator in **a** the off and **b** the on states
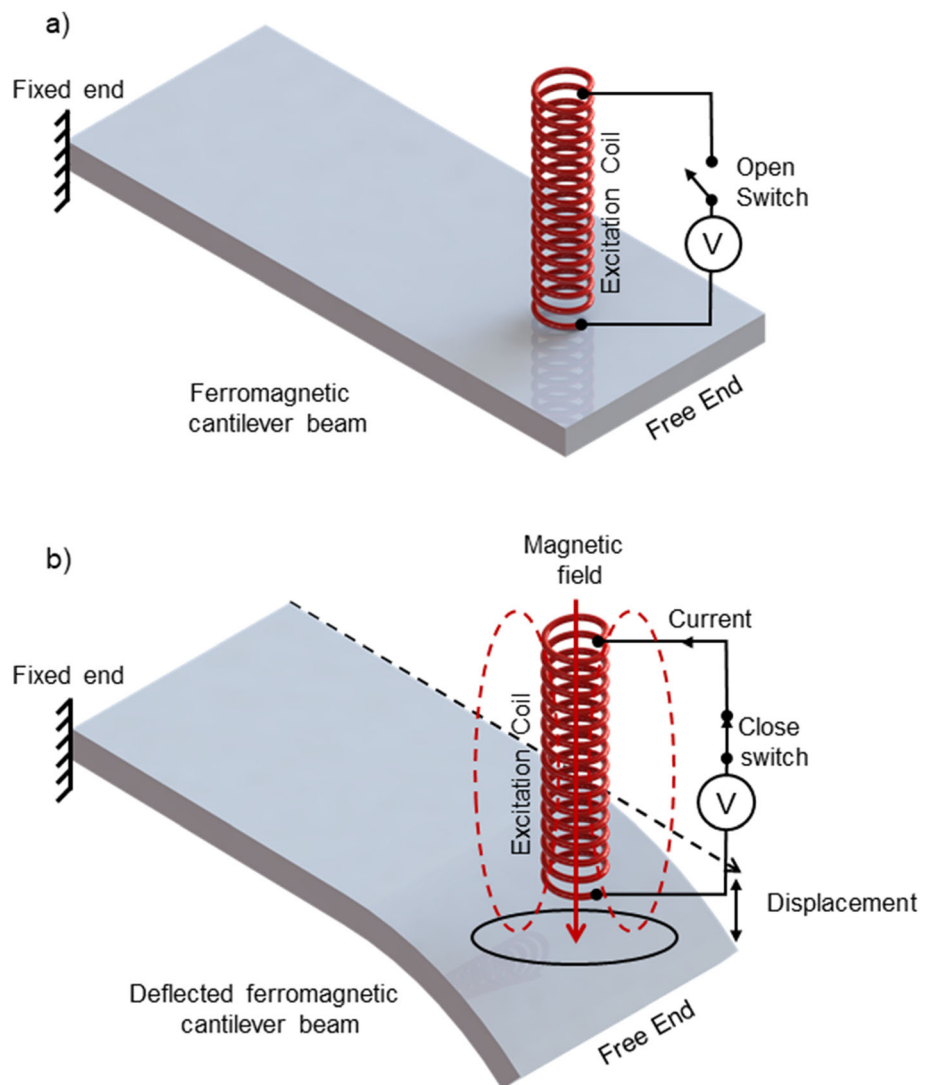
$$X = \frac{12FL^3}{8Ewt^3} \tag{3}$$

where L, E, w, and t are the length of the beam, Young's modulus of the material, the width of the beam, and the thickness of the beam, respectively.

In the case of magnetostriction, a ferromagnetic material is subjected to a magnetic field and the magnetostrictive effect causes the material to change shape. Previously, Singh et al. developed a stress compensated magnetic actuator using a bilayer consisting of silicon dioxide (SiO_2) and magnetostrictive iron-cobalt (Fe65Co35) thin films that resulted in a deflection of 162.75 nm (Singh et al. 2019). Gu-Stoppel et al. incorporated a neodymium (NdFeB) permanent magnet for actuation. Even a single micro magnet or a micro-magnet array can be made into any shape and mounted on actuators with great flexibility (Gu-Stoppel et al. 2019). Over the years, NdFeB magnets have become the most frequently used material for

magnetic actuators, as shown in Table 2. Due to the relatively low output force of most magnetic actuator applications, they are particularly well suited for use in surgical equipment. Furthermore, the magnetic actuator has a fast response time and a large displacement appropriate to the actuator size. Due to their advantages such as simple drive mode, high field energy density, fast response time, and significant deflection achievable with low input voltages, this type of actuator is favorable in several MEMS-based biomedical applications (Kim et al. 2005; Lee et al. 2009). Microgrippers (Ullrich et al. 2015), micropumps (Gidde et al. 2019; Zhou and Amirouche 2011), and surgical tools (Di Natali et al. 2015; Forbrigger et al. 2019) are among their many uses. However, common flaws in electromagnetic actuators include parasitic loss at high frequencies and a rapid decline in volumetric scaling of produced electromagnetic forces as the system size shrinks (Ceyssens et al. 2019).

Table 2 Performance of magnetic actuator

Material	Dimension (mm)		Displacement (mm)	Magnetic flux (T)	Actuation frequency (Hz)	Force (N)	References
	Diameter	Length					
Magnetic coils	6	12	NA	NA	4	7 m	Lee et al. (2014a, b)
Nitinol, NdFeB magnet	4	21	< 0.2	20 mT	60	6 m	Forbrigger et al. (2019)
Nitinol, permanent magnet	8.5	18.5	300 μm	15 mT	NA	0.1	Ullrich et al. (2015)
PDMS, electromagnetic inductive coil	6	0.5	NA	NA	45	75 m	Gidde et al. (2019)
PDMS, NdFeB magnet	7	0.45	NA	NA	36.9	23.7 m	Zhou and Amirouche (2011)
MaxiMag low-carbon iron, NdFeB magnet	10	31	1.5 mm	2	NA	6.8	Wang and El Wahed (2020)
NdFeB magnet	15	30	NA	NA	NA	5	Di Natali et al. (2015)
Silicon Dioxide (SiO2), Iron-Cobalt (Fe65Co35)	76	0.578	162.75 nm	NA	25.3	NA	Singh et al. (2019)
NdFeB magnet, epoxy, Cu, silicon substrate	300 μm	NA	770 μm	40 mT	NA	4.3 m	Wang et al. (2021)
SiO_2, Al, permanent magnet	NA	NA	55 μm	0.14 T	1.2 k	NA	Lv et al. (2015)
NdFeB magnet	4	NA	10–50 μm	14 mT	1	0.01 m	Imai and Tsukioka (2014)
Nd, Ce, Fe, B, PDMS	130 μm	2	600 μm	7 mT	NA	NA	Rahbar and Gray (2017)
NiFe alloy	NA	5.1	5.4 mm	NA	200	NA	Jia et al. (2021)
NdFeB magnet, Silicon (Si)	2	500 μ	323 μm	500 mT	NA	10.1 m	Gu-Stoppel et al. (2019)
NdFeB powder, PDMS	NA	12	100 μm	16.8 T	NA	2.2 m	Qi et al. (2021)
NdFeB magnet, Si	3	1.5	2.75 μm	NA	0.025	2.5 m	Pawinanto et al. (2016)
Single crystal silicon	NA	2.7	150 μm	0.48 T	NA	1 μ	Park et al. (2017)

2.3 Piezoelectric actuation

Even though thermo-responsive and magnetic actuation produce high output forces, their positioning resolution, response time, and accuracy are inadequate. As a result, they do not meet the requirements for biomedical applications that necessitate precise control, rapid response, and accuracy, such as surgical instruments. Piezoelectric actuators, on the other hand, are of great significance because they possess advantages such as fast response, good operating bandwidth, compact size, and low power consumption (Gao et al. 2020; Ghazali et al. 2020; Nikpourian et al. 2019). Thus, they are often utilized in applications that require high-precision actuation such as micro/nano-positioning systems (Chen et al. 2016), micropumps (Ma et al. 2015a, b; Ma et al. 2015a, b), and microgrippers (Chen et al. 2020; Li et al. 2018).

Piezoelectric actuators operate using the converse piezoelectric effect of a piezoelectric crystal to induce strain by supplying an electric voltage to the crystalline material. The converse piezoelectric effect can be defined by Eqs. (4) and (5), where the mechanical strain (S) and displacement density (D) are combined with mechanical stress (T) and the electrical field (E) (Janocha 2004):

$$S = s^E T + dE \qquad (4)$$

$$D = dT + \varepsilon^T E \qquad (5)$$

where s^E, T, d, and ε represent compliance coefficient for constant E, mechanical stress, piezoelectric charge constant, and dielectric constant of a piezoelectric material, respectively. The mechanism of operation of this type of actuator largely depends on the crystal orientation of the piezoelectric material. In the absence of E and when operated above the Curie point, the temperature at which a material loses its spontaneous polarization and piezoelectric properties, electrical dipoles in the piezoelectric material are randomly oriented. The material leaves the property of piezoelectricity in this state, and no strain is induced. The piezoelectric crystal regains the property of piezoelectricity below the Curie point. When E is applied parallel to the piezoelectric crystal, the electrical dipoles align near the applied field. It then triggers the asymmetric axis of the material and allows it to elongate in the direction of E. This effect is known as the polarization effect. Depending on the polarization field (P) and E, the piezoelectric actuator can be deformed into three actuation modes, i.e., longitudinal, transverse, and shear. Actuation modes with the direction of P for a single layer of piezoelectric crystal are shown in Fig. 5. Without applied E, there is no strain in the piezoelectric actuator, as illustrated in Fig. 5a. In the case of longitudinal and transverse modes, E is applied parallel to P resulting in longitudinal deformation (δh) (Fig. 5b) and transversal deformation (δl) (Fig. 5c). However, when E is placed perpendicular to P for shear mode, it results in a shear deformation (δs) (Fig. 5d) (Peng and Chen 2013).

As shown in Fig. 6, piezoelectric actuators can be classified into two types based on their structural design, namely unimorph and bimorph actuators. The unimorph piezoelectric actuator is a cantilever consisting of a single piezoelectric material and an elastic layer. In contrast, an elastic layer is sandwiched by two piezoelectric material layers in a bimorph structure (Wang and Cross 1998). In the unimorph actuator, when E is subjected to the piezoelectric layer, it is operated to expand or contract and the elastic layer prevents the dimension change, resulting in both bending and stretching. For example, Srinivasa Rao et al. (2020) fabricated an actuator using a PDMS diaphragm and a lead zirconate titanate (PZT) layer. Gunda et al. developed a PZT unimorph micro-actuator in which an active piezoelectric layer (PZT-5H, Piezo Systems T105-H4E-602 [12]) and the stainless-steel passive layer were bonded with conductive epoxy. The active layer exhibits inward lateral displacement due to the inverse piezoelectric effect, which creates a bending moment that forces the stainless steel membrane downward (Gunda et al. 2020). Furthermore, Munas et al. proposed circular PZT actuated metal diaphragms as micropump actuators. With alternating voltage, the pumping action (suction and compression strokes) of PZT diaphragms deforms in a concave (suction) and convex (compression) manner (Munas et al. 2018).

On the contrary, one-layer contracts while the other expands, resulting in the bending deformation of the bimorph actuator. Liu created a poly (vinylidene fluoride) (PVDF) piezoelectric bimorph actuator by sandwiching its sheets of PVDF electrode and aluminum foil. The developed actuator demonstrated bimorph bending in response to an electric field, with one sheet shrinking in length and the other expanding (Liu et al. 2019). Table 3 presents the performance of various piezoelectric actuators mainly composed of PZT and polymethyl methacrylate (PMMA). Most of these piezoelectric actuators have been used in microfluidic systems (e.g., micropump and microvalve systems) because of their simple structure, fast response, and good energy conversion efficiency. As can be seen in the table, the frequency of the piezoelectric actuator has a comparatively significant value, implying a faster response time.

2.4 Soft actuation

The term "soft actuation" refers to actuators made of elastomer or rubber materials. Akin to pneumatic actuators, electroactive polymers (EAP) and HASEL are also

Fig. 5 Actuation modes of piezoelectric actuators with **a** no supply, **b** longitudinal mode, **c** transversal mode and **d** shear deformation
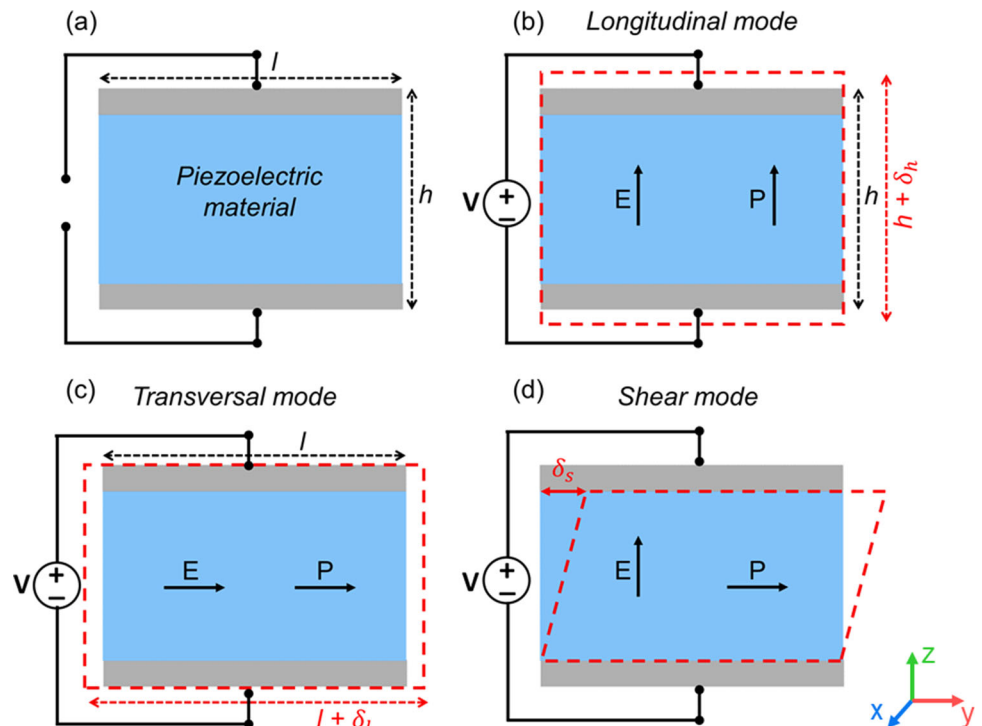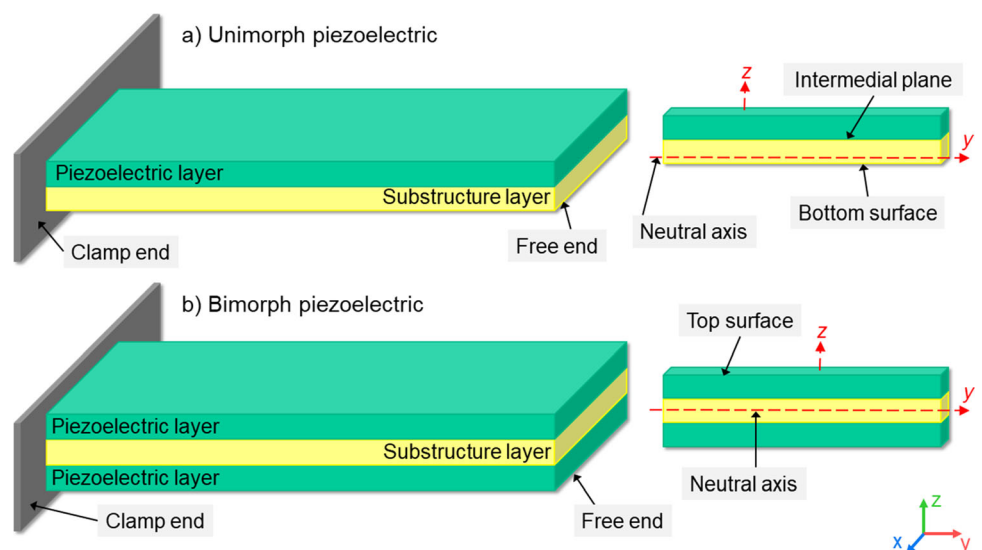

Fig. 6 Types of piezoelectric actuators. **a** Unimorph piezoelectric actuator and **b** bimorph piezoelectric actuator

categorized as soft actuators. Elastomer-based soft actuators have gained enormous popularity due to their high flexibility, high compliance, biocompatibility, lightweight properties, high power-to-weight ratio, low material costs, and ease of fabrication. This section discusses in detail soft actuators such as pneumatic, EAP, and HASEL actuators.

2.4.1 Pneumatic actuator

A pneumatic actuator is a device that uses compressed air to create mechanical motion. Pneumatic soft actuators are typically constructed of a flexible polymer material with a fiberless or fiber-reinforced structure and an internal chamber (or chambers). When pressure is applied to the internal chamber, the actuator deforms to achieve the desired deformation. The actuator's response time depends on the chamber's internal volume, and the elasticity of the elastomer used (Shintake et al. 2018a, b). Pneumatic actuators provide linear expansion, bending, and twisting motions depending on the actuators' design, as shown in Fig. 7 (Digumarti et al. 2017; Ge et al. 2018; Gorissen et al. 2014).

Table 3 Performance of piezoelectric actuator

Material	Dimension (mm)	Driving voltage (V_{pp})	Displacement (mm)	Actuation frequency (Hz)	References
PZT, polymethyl methacrylate (PMMA)	65 × 40	19.4	40 μm	15	Zhang et al. (2013)
NA	140 × 100	13	40 nm	3.5 k	Zhang et al. (2018)
PZT, Al	46.5 × 45.12	150	924 μm	NA	Chen et al. (2020)
PZT, Al	Length: 150 Diameter: 1.7	6	10	0.1	Li et al. (2018)
PZT, PMMA	4.5 × 1.3	50	NA	200	Junwu et al. (2005)
PZT, PMMA, PDMS, SU-8, parylene C	15 × 8	36	NA	200	Liu et al. (2010)
PZT, PMMA	40 × 40	150	NA	22	Zhang et al. (2016)
PZT, PMMA	Thickness: 0.3 Diameter: 35	20	NA	100	Munas et al. (2018)
PZT, Cu	Length: 17	140	19.3	0.8 m	Na et al. (2018)
PZT, polyactic acid (PLA)	60 × 45	210	NA	49	Zhang et al. (2020)
PZT, Al	66.2 × 22	150	150 μm	0.2	Das et al. (2020)
PZT, PDMS	23 × 23	230	NA	75	Pečar et al. (2014)
PZT, PLA	NA	210	NA	120	Peng et al. (2019)
PZT, PLA	L 60 × H 42 Diameter: 35	220	0.6	45	Zhao et al. (2019)
PZT, PMMA	5 × 5 × 20	150	153 μm	5	Mohith et al. (2020)
PZT, PLA	70 × 42 Diameter: 35	190	NA	130	He et al. (2019)
PZT, PMMA, PDMS	22	7	NA	10 k	Nafea et al. (2018)

As illustrated in Fig. 7, pneumatic actuator movements can be divided into two types: symmetric and asymmetric movements. The symmetric cross-section can expand or contract in response to the pneumatic force applied (Belding et al. 2018; Byrne et al. 2018). The asymmetric cross-section shows bending formations resulting from the bonding of two layers, such as a pneumatic balloon actuator (PBA) with different thicknesses or elasticities (Shintake et al. 2017). Meanwhile, twisting motions are triggered by the simultaneous activation of two combined arrays of PBAs in the opposite bending directions (Gorissen et al. 2014). These motions are the results of the actuation mechanism where pneumatic input is applied to the actuator's channel causing elastic deformation (contraction or expansion) in its structure, resulting in actuation (bending or twisting motion) (Agarwal et al. 2016; De Volder and Reynaerts 2010; Xavier et al. 2021).

Furthermore, pneumatic actuators (PSA) offer a bidirectional or curling motion (Razif et al. 2014; Rehman et al. 2019; Suzumori et al. 2007) depending on the fabricated channel structure (single or dual configuration). Wakimoto et al. (2009a, b) developed a three-channeled pneumatic soft actuator that showed bending motions in six different directions. Based on the positive features of PSA, Suzumori (1996) developed a three-DoF (pitch, yaw, and stretch) flexible micro-actuator consisting of a cylindrical fiber-reinforced rubber structure to prevent the actuator from deformation in the radial direction, and three internal chambers for pneumatic supply. Overall, pneumatic actuators offer a number of advantages, including high displacement, biocompatibility, lightweight design, high power-to-weight ratio, and ease of fabrication. Due to their characteristics, pneumatic actuators are well-suited for surgical and gripper applications. Nonetheless, pneumatic

Fig. 7 Pneumatic actuators. **a** Symmetric cross-sections with expanding motion Reproduced with permission from Belding et al. (2018), Wiley–VCH. Asymmetric cross-sections with **b** twisting motion. Reproduced with permission from Gorissen et al. (2014), Elsevier. **c** Bending motion. Reproduced with permission from Xavier et al. (2021), Elsevier
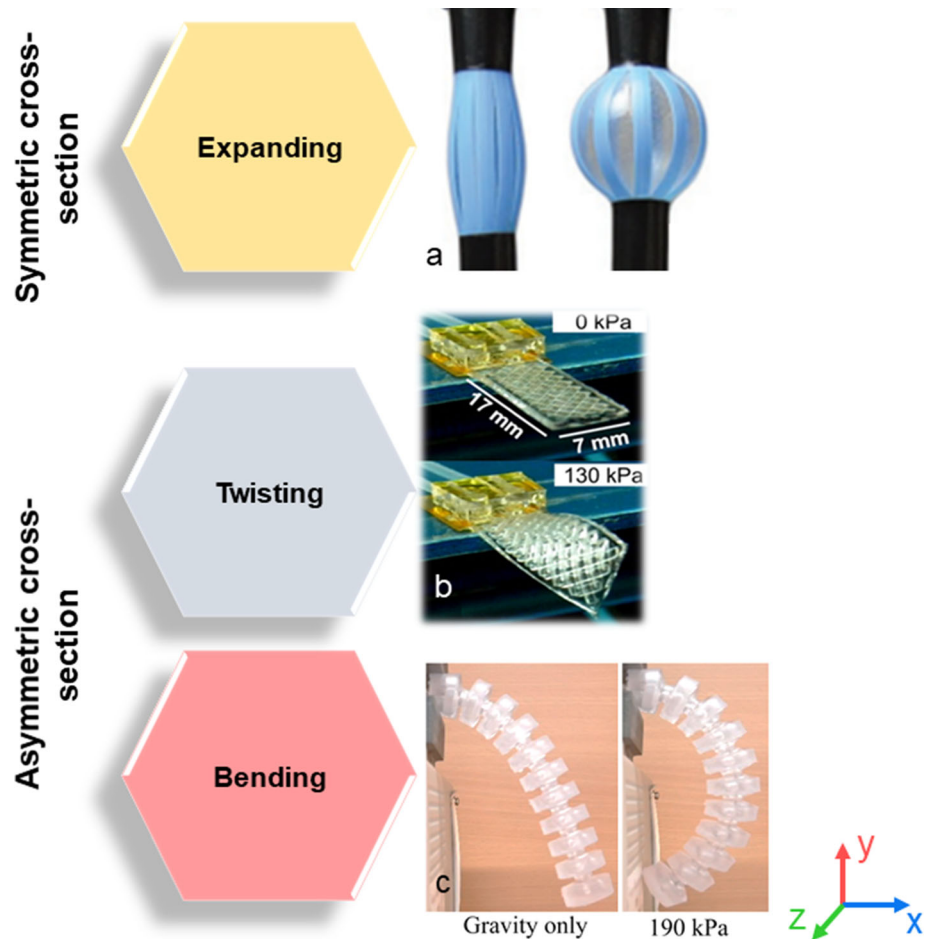
actuators have a few limitations such as low actuation accuracy and a large overall size.

2.4.2 Electroactive polymer actuator

Ionic polymer-metal composite (IPMC) and dielectric elastomer (DE) are classified as EAP actuators, as the polymers have the ability to deform when triggered by electrical stimuli. EAP can be categorized into two major classes, namely ionic EAP (e.g., IPMCs, conducting, and carbon nanotubes) and field activated EAP (e.g., ferroelectric and DE) based on their activation mechanism. This section focuses on IPMCs and dielectric elastomer actuators (DEA), the most widespread actuators among ionic and field activated EAPs technologies utilized in biomedical devices as well as the robotics field (Anderson et al. 2012; Jo et al. 2013; Rosset and Shea 2016; Shahinpoor and Kim 2004).

2.4.2.1 Ionic polymer metal-composite actuator The IPMC has been widely studied as an ionic EAP material for its advantageous properties including considerable bending strain, low power consumption, good flexibility, and low

activation voltage. These characteristics have increased the demand for the development of IPMC in soft robotics and other industrial fields, as they are suitable for applications in drug delivery, optical systems, and soft grippers. IPMC is composed of three layers of a sandwich-like structure with a thin electrolyte membrane plated by noble metal electrode layers on each side of the base membrane (Shahinpoor and Kim 2001). Due to their similar chemical structure and properties, Nafion, Flemion, and Aciplex are the most commonly used materials for electrolyte base membranes. The conductive layer, which is plated on both sides of the base membrane, is made up of a mix of noble metals such as gold, platinum, or palladium.

The working mechanism of IPMC is illustrated in Fig. 8. In a neutral state, the anions and cations in the polymer membrane are distributed evenly. On the contrary, when an electric field is applied to the IPMC, the cations together with water molecules will migrate toward the cathode. Strain then occurs near the IPMC's cathode due to anisotropic concentration distributions of cations and water molecules, and differential swelling leads to the IPMC bending toward the anode (Park et al. 2008; Schmidt-Rohr and Chen 2008; Shahinpoor 2003; Sun et al. 2013).

Fig. 8 Mechanical operation of IPMC

Hydrated cations   Water molecule   Fixed anions
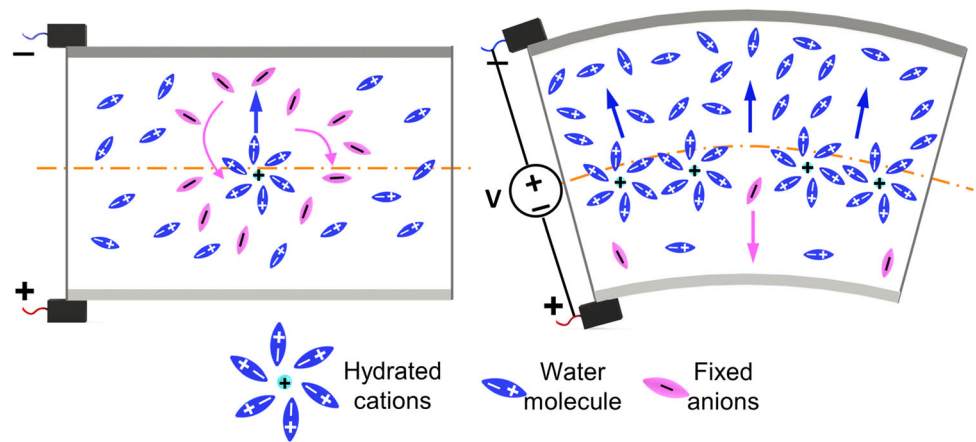
Although IPMCs demonstrate the aforementioned beneficial properties, they frequently suffer from slow response, low electromechanical coupling efficiency, the need to maintain electrolytes, and the inability to sustain constant displacement under activation of a DC voltage (except for conductive polymers).

2.4.2.2 Dielectric elastomer actuator As a type of EAP, DEA has been widely adopted in the biomedical and robotic fields, (Pelrine et al. 2000) in which electrically actuated elastomers have been reported to have enormous strains and high electromechanical transduction efficiency. DEA has been utilized in MEMS biomedical outside-of-the-body applications (Ghazali et al. 2017; Qin et al. 2018; Wu et al. 2021). This is due to DEA's favorable features such as high mechanical energy density, reconfigurability, high efficiency, high strains, fast response time, and self-sensing characteristics (Ashley 2003; Keplinger et al. 2012; Kwon et al. 2008; Maffli et al. 2015; Rosset et al. 2013). In addition, DEA is well known for its excellent electromechanical performance and convenience of electrical control. However, despite its superior performance, DEA needs a very high voltage for actuation. Furthermore, DEA requires rigid frames and pre-stretched materials to produce significant strains upon activation, which limits its DoF (Zhao and Suo 2010). Moreover, because DEA needs stretchable dielectric layers, (Rosset and Shea 2013) elastomer membranes frequently suffer from mechanical fatigue and degradation under high strains (de Saint-Aubin et al. 2018; Zhang et al. 2019a, b, c). Other than biomedical applications (Brochu and Pei 2012; Sheima et al. 2019), soft robotic (Araromi et al. 2014; Heng et al. 2017; Kofod et al. 2007), and robotic locomotion or movements (Nguyen et al. 2017; Pei et al. 2004; Shintake et al. 2018a, b; Tang et al. 2017) are among the common applications of DEAs.

The actuator's operation is based on electromechanical actuation, which is achieved when a high voltage is supplied across the electrodes, causing a potential difference that generates compressive electrostatic forces (also known as Maxwell stress) between them. The compressive force causes thickness reduction and lateral expansion of the elastomer membrane, as shown in Fig. 9.

The electrostatic force present on the flexible membrane can be correlated with the driving voltage, V, DE membrane thickness, d, and the surface area, A. The electrostatic force of the flexible membrane, F_e, is expressed in the Eq. (6):

$$F_e = \frac{1}{2}\varepsilon\left(\frac{V}{d}\right)^2 A = \frac{1}{2}\varepsilon_o\varepsilon_r V^2 \left(\frac{1}{D_o - w}\right)^2 A \qquad (6)$$

where ε is the dielectric constant of the DEA, ε_o is the permittivity of free space, ε_r is the relative dielectric constant of DEA, D_o is the initial displacement between the electrodes, and w is the displacement in the transverse z-direction. According to Bigué and Plante (2011) the structural deformation is caused by Maxwell stresses induced by electric charges on the electrodes. The total electric charges, Q, on the electrodes under voltage, V, are given by:

$$Q = CV \qquad (7)$$

As per Hill et al. (2017) by treating the DE membrane as a parallel plate capacitor, the actuator capacitance, C can be expressed as:

$$C = \varepsilon\frac{A}{d} \qquad (8)$$

Essentially, the charges obtained from Eq. (7) and the capacitance calculated from Eq. (8) allow for the calculation of the electrostatic force on the DE membrane, as represented by Eq. (6). Then, the Maxwell pressure, P, which acts across the two electrodes due to the electrostatic attraction is given by:

Fig. 9 Schematic diagram of DEA working mechanism
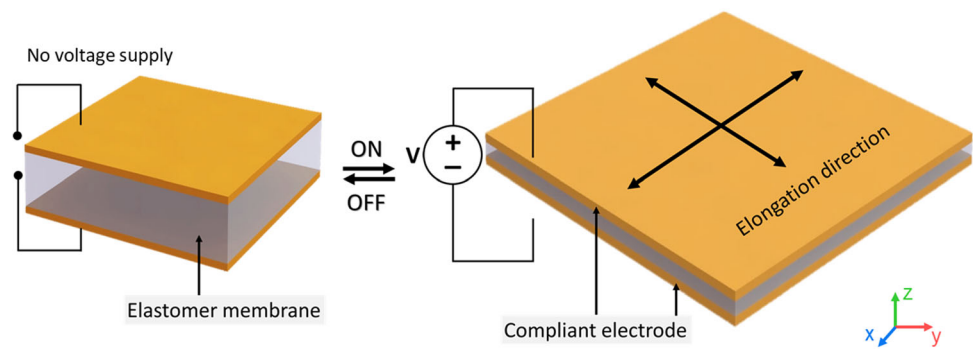
$$P = \varepsilon_r \varepsilon_0 \left(\frac{V}{d}\right)^2 \tag{9}$$

Dielectric elastomer soft actuators are commonly made of silicone elastomers, polyurethanes (PUs), and acrylic elastomers (3M VHB 4910 and VHB 4905). Acrylic elastomers, such as the widely used VHB4910 elastomer, can deform significantly. However, they are extremely viscoelastic, limiting the actuator's displacement bandwidth. Silicone and PU-based elastomers, on the other hand, have a faster frequency response. They can be cast into various shapes, even though the resulting strain is significantly lower than that of acrylic elastomers.

2.4.3 Hydraulically amplified self-healing electrostatic actuator (HASEL)

Hydraulically amplified self-healing electrostatic actuator (HASEL) is a novel technology derived from the combination of DEA and fluid-driven soft actuator technologies while addressing DEA drawbacks. HASEL has a significant advantage over DEA in terms of displacement and is extremely versatile, as it can achieve all basic actuation modes (expansion, contraction, and rotation). They can also self-sense their deformation state and be produced from various materials with a wide range of form factors and sizes. HASEL actuator consists of a deformable flexible shell filled with a liquid dielectric covered with a pair of compliant electrodes. When voltage is applied to the electrodes, an electric field is generated through the dielectric fluid. As a result, Maxwell stress acts on the elastomeric shells and causes the dielectric fluid to be displaced from between the opposing electrodes to the surrounding area, which effectuates a shape change of the soft hydraulic structure (Fig. 10).

HASEL actuators have been utilizing silicone elastomers and thermoplastic polymers as their elastomeric shells. Silicone elastomers have attractive features such as favorable dielectric properties, dielectric breakdown strength of up to $\approx 50 - 120 \mathrm{kVmm}^{-1}$, high stretchability, and resilience to damage (Madsen et al. 2014;

Vaicekauskaite et al. 2020). However, Acome et al. (2018) created a distinctly different design of HASEL actuator called the elastomeric donut HASEL (Fig. 10a) and planar HASEL (Fig. 10b). As mentioned in the name, the "donut" shape is the result formed when voltage is applied to the actuator; comprised of a circular shell filled with dielectric liquid with a pair of circular electrodes placed concentrically on both sides of the shell resulting in the deformation of the initial shapes causing an increase in the height of the overall elastomeric donut actuators. Planar geometry for planar HASEL, on the other hand, is based on a flexible dielectric shell coated with compliant electrodes and filled with a liquid dielectric that expands in-plane when activated. According to the analysis, planar HASEL behaves similarly to DEA in terms of actuation; however, the fluid in planar HASEL reduces stiffness and allows it to attain larger strains than DEA of the same dimensions (Acome et al. 2018).

However, elastomer-based materials have several drawbacks including the lack of material choice (high-quality elastomeric films), dielectric fluid leakage during actuation, and stretchable electrodes leading to lengthy fabrication procedures. The introduction of thermoplastic materials, such as biaxially oriented polypropylene (BOPP) films, avoided the many drawbacks of stretchable dielectrics and electrodes, such as limited material selection and device reliability (de Saint-Aubin et al. 2018; Kornbluh et al. 2012; Rosset and Shea 2013). It also enabled a significant Maxwell stress with breakdown strengths of nearly 700 kVmm^{-1}, a host of new actuation geometries, fabrication methods, and performance capabilities in HASEL actuators (Mitchell et al. 2019; Rothemund et al. 2021). Apart from donut shaped and planar HASEL, Kellaris et al. (2018) developed Peano-HASEL by combining the electrostatic principles of elastomeric HASEL actuators (Acome et al. 2018) with the strength of linearly contracting Peano-fluidic actuators created by Niiyama et al. (2015) and Sanan et al. (2014).

Peano-HASEL actuators are a type of soft electrohydraulic transducer with a fast linear contraction on activation and high force production and scalability. According

Fig. 10 Actuation mechanism of **a** donut shaped HASEL and **b** planar HASEL
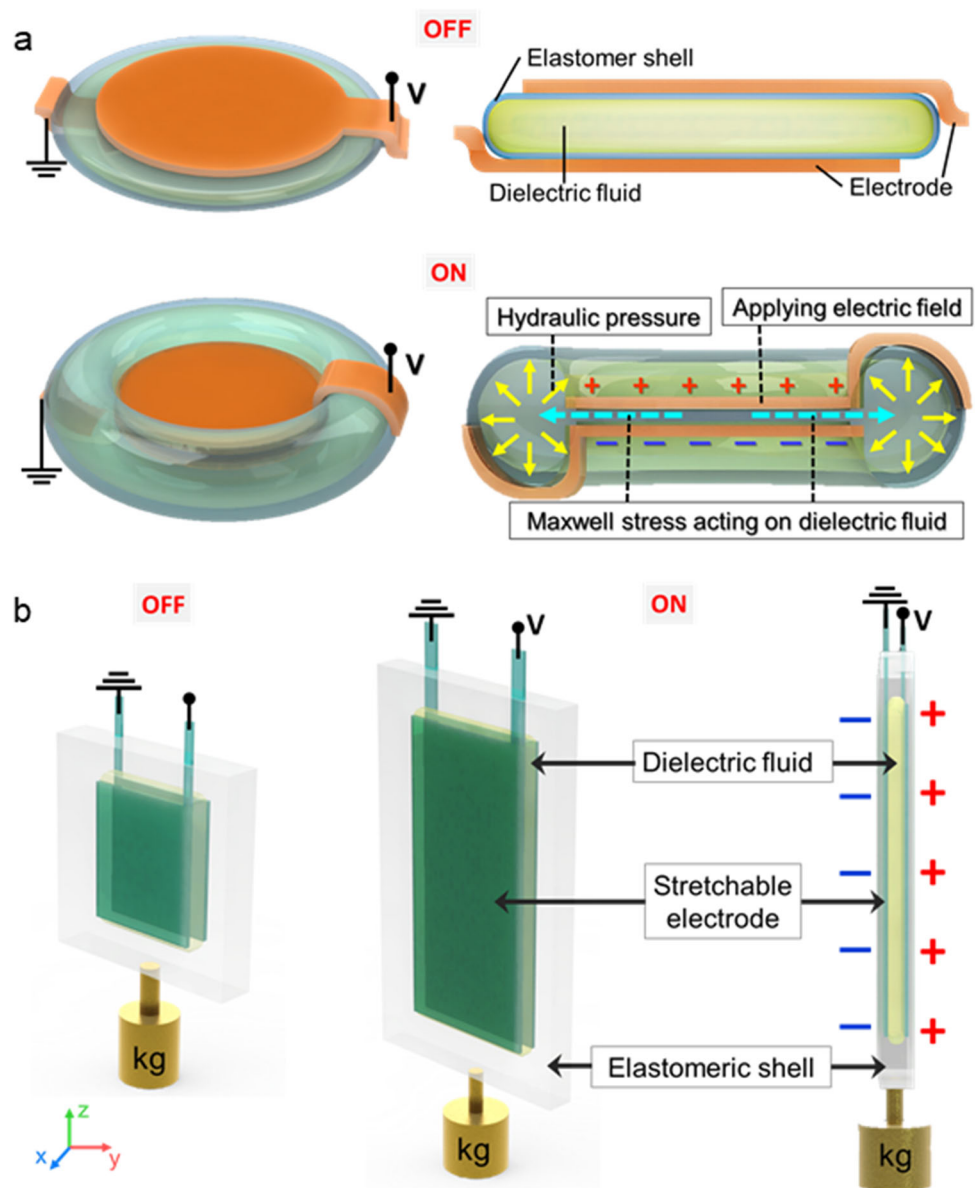
to Rothemund et al. (2019), the basic configuration of the Peano-HASEL actuators consists of rectangular shells shaped by inextensible but flexible polymer film bonding. Peano-HASEL actuators were investigated using the same thermoplastic as HASEL actuators, where the linear contraction of soft electrostatic actuators occurs without the need for pre-stretch, rigid frames, or stacked configuration (Rothemund et al. 2021). These shells are filled with a liquid dielectric and sealed to form a pouch, with a pair of opposing electrodes placed on both sides, covering a section of the shell. When voltage is applied between the electrodes, the resulting electric field allows the electrodes to zip together against one another, beginning at the edge of the shell where the electrodes are closest to one another, and the electrical field is strongest. As a result, the zip

electrodes shift the liquid dielectric into the shell area that the electrodes do not cover. Furthermore, the hydrostatic pressure inside the shell rises due to the shell's inextensibility and the non-compressibility of the liquid dielectric, causing the actuator to contract linearly (Fig. 11d). Nevertheless, Peano-HASEL has 15% strain limitations, whereas the average strain of skeletal muscle is around 20%. As a result, Wang et al. developed an improved approach known as high-strain (HS) Peano-HASEL actuator, which overcame this problem by placing electrodes on the sides of each shell. When a voltage is applied, contraction occurs as the electrodes zip from the shell's side, forcing the liquid dielectric towards the actuator's center (Fig. 11c). As a result, the HS Peano-HASEL actuator can
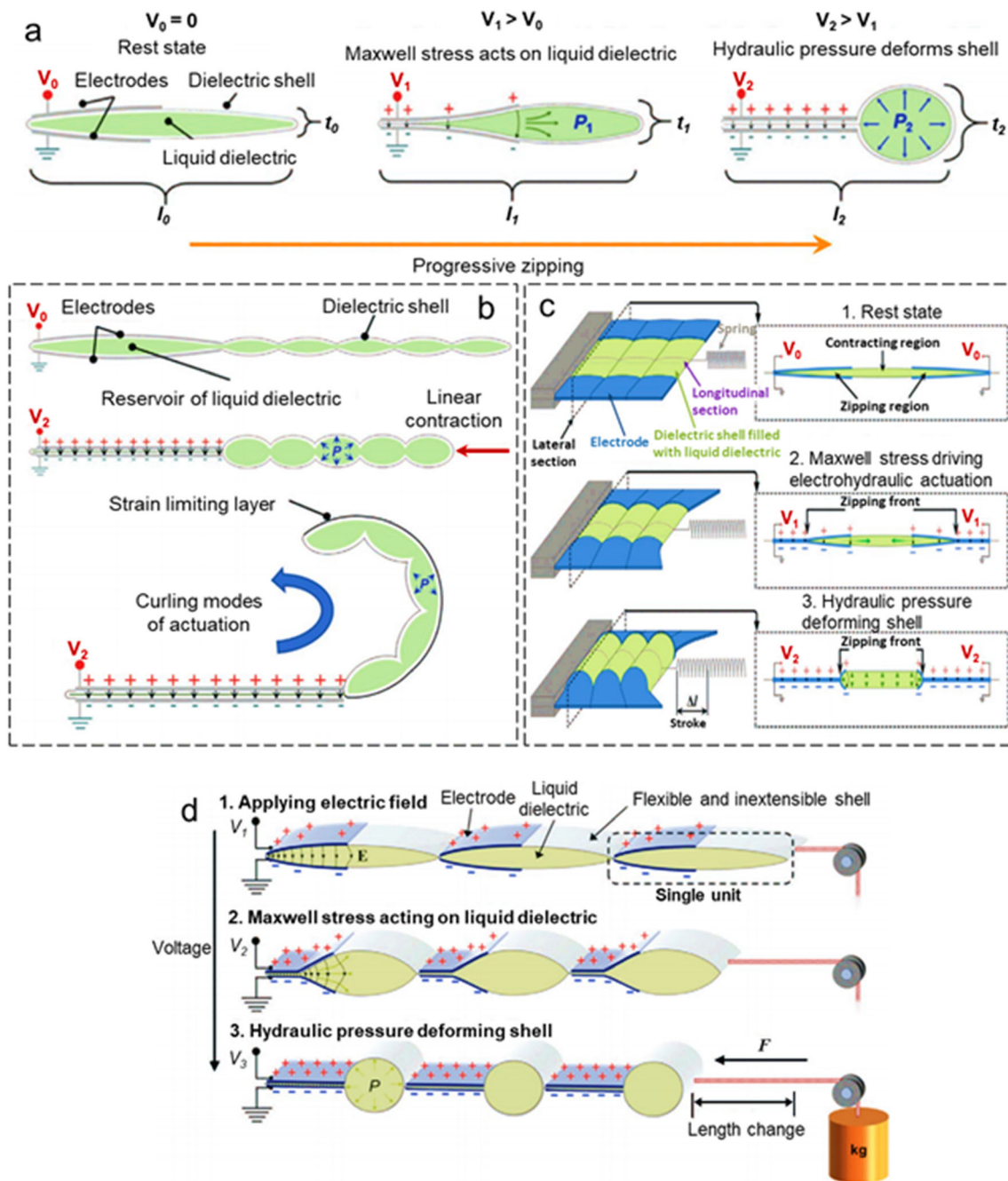
Fig. 11 Working mechanism of **a** quadrant donut HASEL, **b** curling HASEL, **c** high-strain Peano-HASEL, and **d** Peano-HASEL. Reproduced with permission from Ref. [180]. Copyright 2021, Wiley–VCH

provide more strain while requiring less blocking force (Wang et al. 2020).

Peano-HASEL not only exhibits linear contraction but also thickness expansion, resulting in the configuration of a quadrant donut HASEL actuator with controlled linear expansion (Rothemund et al. 2021). The quadrant donut actuator comprises of a circular thermoplastic shell covered by circular electrodes on both sides at the center of the actuator. There are heat seals in the four separate quadrants

of the shell. This heat seal creates a zipping initiation to avoid the pull-in instability in the elastomeric donut HASEL actuator (Fig. 11a). Other than that, motivated by hydraulic actuation found in species of arachnids (Spagna and Peattie 2012), a prototype of bioinspired designs of HASEL actuators that contract, curl, or twist was reported (Rothemund et al. 2021). The shell of these actuators consists of a large, electrode-covered chamber, which acts as a reservoir of liquid dielectric connected to a corrugated

Table 4 Performance of soft actuator

Type of actuation	Dimension (mm)		Displacement (mm)	Force (N)	Pressure (Pa)	Actuation frequency (Hz)	References
	Diameter	Length					
Pneumatic	32	135	10	2.2	0.06 M	NA	Ranzani et al. (2015)
Pneumatic	2.4	9	NA	0.5	55 k	NA	Guo et al. (2017)
Pneumatic	1	10	NA	NA	280 k	14	Gorissen et al. (2018)
Pneumatic	12	120	20.7	50 m	0.2 M	NA	Wakimoto et al. (2009a, b)
Pneumatic	3.5	65	14	0.45	130 k	NA	Zhang et al. (2019a, b, c)
Pneumatic	NA	27.6	NA	0.22	100 k	NA	Rehman et al. (2019)
Pneumatic	NA	1170	47	190	758 k	NA	Ohta et al. (2018)
Thermo-pneumatic	2	20	65 μm	NA	NA	NA	Hamid et al. (2017)
Pneumatic	20	60	7	NA	600 k	NA	Sun et al. (2019)
Pneumatic	25	30	10	120	137 k	8	Naclerio and Hawkes (2020)
Pneumatic	1.3	24.6	95	NA	400 k	NA	Liu et al. (2020)
IPMC	10	35	3.3	50 m	NA	NA	McDaid et al. (2012)
IPMC	12.8	58	NA	NA	2.3 k	0.4	Kalyonov et al. (2020)
IPMC	NA	9	0.043	NA	NA	0.025	Chang et al. (2018a, b)
IPMC	1	25	1.67	NA	NA	0.1	Horiuchi et al. (2017)
IPMC	NA	8	0.043	NA	NA	0.025	Chang et al. (2018a, b)
DEA	NA	NA	30 μm	3	NA	5	Lee et al. (2017)
DEA	6	40	0.42	NA	NA	3	Ghazali et al. (2017)
DEA	10	NA	2.6	NA	193 h	102.1	Linnebach et al. (2020)
DEA	5	10	200 μm	40 m	NA	5	Lee et al. (2014a, b)
DEA	NA	15	33.8 μm	NA	NA	10	Solano-Arana et al. (2018)
HASEL	NA	80	1.39	18	2.73 k	40	Wang et al. (2020)

structure of smaller chambers (Fig. 11b). Upon activation, the liquid dielectric is forced from the reservoir into the corrugated structure; the radius of curvature decreases and the structure contracts linearly. The curling motion can be accomplished by applying a strain-limiting layer to one side of the actuator, which stops corrugations from contracting on that side. As a result, it contributes to the curling of the corrugated structure away from the strain-limiting layer applied to the actuator.

Table 4 shows the performance of the previously reported DEA as well as pneumatic, IPMC, DEA, and HASEL actuators. According to the results of the analysis, soft actuation has a fast reaction time in general, with the exception of the IPMC actuator, which has the lowest frequency. Furthermore, the overall force of the pneumatic actuator is greater than that of the IPMC, DEA, and HASEL actuators. Nonetheless, DEA actuators have a higher actuation frequency than pneumatic, IPMC, and HASEL actuators. The average soft actuation displacement was large in comparison to their size, with the pneumatic actuator delivering a comparatively high displacement.

Nonetheless, the major drawbacks of pneumatic, IPMC, and DEA actuators are their slow response and degradation over time. To address these shortcomings, researchers investigated HASEL actuators which use dielectric fluid to prevent charge dissipation and thus enable a faster response with significant actuation deflection.

3 Biomedical applications

This section focuses on the use of thermo-responsive, piezoelectric, magnetic, and soft actuators in biomedical applications. Biomedical actuator applications are closely related to movable devices outside of the patients' body, including drug delivery systems, surgical devices, and artificial muscle. The key functionalities of the reported devices as well as their specific contributions are explored.

3.1 Drug delivery systems

Micropumps and microvalves are crucial elements in drug delivery systems to precisely manage medication dosages. As a result of recent advancements in BioMEMS and miniaturization technologies, various biomedical devices have been developed for drug delivery applications (Hilt and Peppas 2005). With the help of actuators, it can deliver a specific type of drug with optimal therapeutic efficacy, eventually assisting in diagnosing and treating chronic and acute diseases (Paul et al. 2016). Moreover, micropumps play an imperative role in drug delivery devices that manipulate drugs or therapeutic agents through channels while transferring them from reservoirs to specific locations accurately and reliably (Amirouche et al. 2009). Usually, the micropump systems use moving elements to manipulate fluid containing drugs and agents by applying pressure in the tens of the kPa range. With the aid of the actuators, micropumps with high actuation pressure forces have been developed for drug flow.

Thermo-responsive actuators, particularly SMA, have been widely employed in developing various micropumps as they provide high actuation force, large displacement, and high work density. For example, Fong et al. designed and fabricated an implantable drug delivery device with an SMA microfluidic pump operated by a radio signal, as shown in Fig. 12a (Fong et al. 2015). When an external RF electromagnetic field activated the actuator, the temperature of the excited nitinol coil exceeded the threshold temperature, resulting in cantilever-like actuation with a displacement of 125 μm. It was able to dispense 219 nL of test agents from a reservoir. In addition, an SMP-based implantable drug delivery system was developed by Zainal et al., where external RF magnetic fields drove the device. As a result, the heated SMP actuator turned into a soft rubbery state, allowing easy deformation. It achieved a 140 μm actuation range at 44 °C device temperature using 0.05 W RF power and a drug release rate of 0.172 μL/min on average.

Other than that, Benard et al. (1998) developed a micropump with a thin-film titanium nickel (TiNi) that pumped fluid at a flow rate of 50 μL/min at maximum backpressure of 5.3 mbar. Makino et al. (2001) fabricated a TiNi SMA actuated micropump, capable of producing displacement of around 95 μm with a bias pressure of 200 kPa, which led to pumping the working fluid at a rate of 0.4 μL/cycle. Aside from thermo-responsive actuators, electromagnetic actuators have been applied in micropumps, where the actuations have been activated by electromagnetic mechanisms. For instance, Rusli et al. (2018) reported an electromagnetically actuated micropump for bidirectional flow. The dual-chamber microchannel design incorporated a dispersing depth structure to provide bidirectional flow. A permanent magnet was affixed to the thin membrane sheet in each of the dual chambers. The power inductor was given a positive voltage polarity, which attracted the magnet, causing fluid to be expelled through the channel. Meanwhile, negative polarity repelled the magnet and inflated the membrane, allowing fluid to enter the chamber. Thus, the constant change of voltage polarities created a net fluid flow to attract and repel the magnet.

Piezoelectric actuators are another type of actuator widely used in various micropumps to precisely regulate fluid flow. For example, Ma et al. (2015a, b) developed a piezoelectric diaphragm actuated micropump with a maximum deflection greater than 1.1 mm. Likewise, Junwu et al. (2005) designed and fabricated a piezoelectrically actuated high-frequency cantilever-valve pump for drug delivery. The piezoelectric actuator, operated in bending vibration mode, pressurized the fluid in the chamber that led the valves to open and close. Consequently, the fluid was transferred at a flow rate of 3.5 ml/min and 27 kPa back-pressure from the inlet to the outlet with an applied frequency of 200 Hz while maintaining therapeutic efficacy.

Moreover, a disposable piezoelectric micropump for insulin delivery and glucose monitoring was developed by Liu et al. (2010), as illustrated in Fig. 12b. It moved the fluid by creating pressure through a change in the volume of the pump chamber. The device was able to transfer fluid at a rate of 6.23×10^{-5} ml per pulse. In addition to the functioning of fluid flow, several studies have been carried out on piezoelectric micro-pumps for simultaneous fluid flow and sensing purposes. For instance, Zhang et al. (2013) fabricated a piezoelectrically actuated double diaphragm micropump (Fig. 12c). The device performed both fluid transportation functions as well as the self-sensing output flow synchronously via a single piezoelectric element. At an operating frequency of 15 Hz, the device produced a maximum deformation of 40 μm and a fluid flow rate of 45.98 ml/min with a driving voltage of 160 V_{pp}. The same group has reported another simultaneously functioning piezoelectric pump with a bimorph transducer (Fig. 12d). The micropump was able to transfer fluid at a rate of 2.93 mL/min (Zhang et al. 2016).

Microvalves are another key component of drug delivery systems that have been used for accurate dosing. It controls drug flow and prevents drug backflow while sealing various molecules, micro/nanoparticles, and chemical reagents (Cobo et al. 2015; Qian et al. 2020). For instance, Aksoy et al. developed an SMP-based microfluidic valve and demonstrated their use as reagent mixers and peristaltic pumps, as shown in Fig. 13a (Aksoy et al. 2019). The moveable element in the valves was made up of a trilayer consisting of SMP, carbon-silicone heaters beneath,
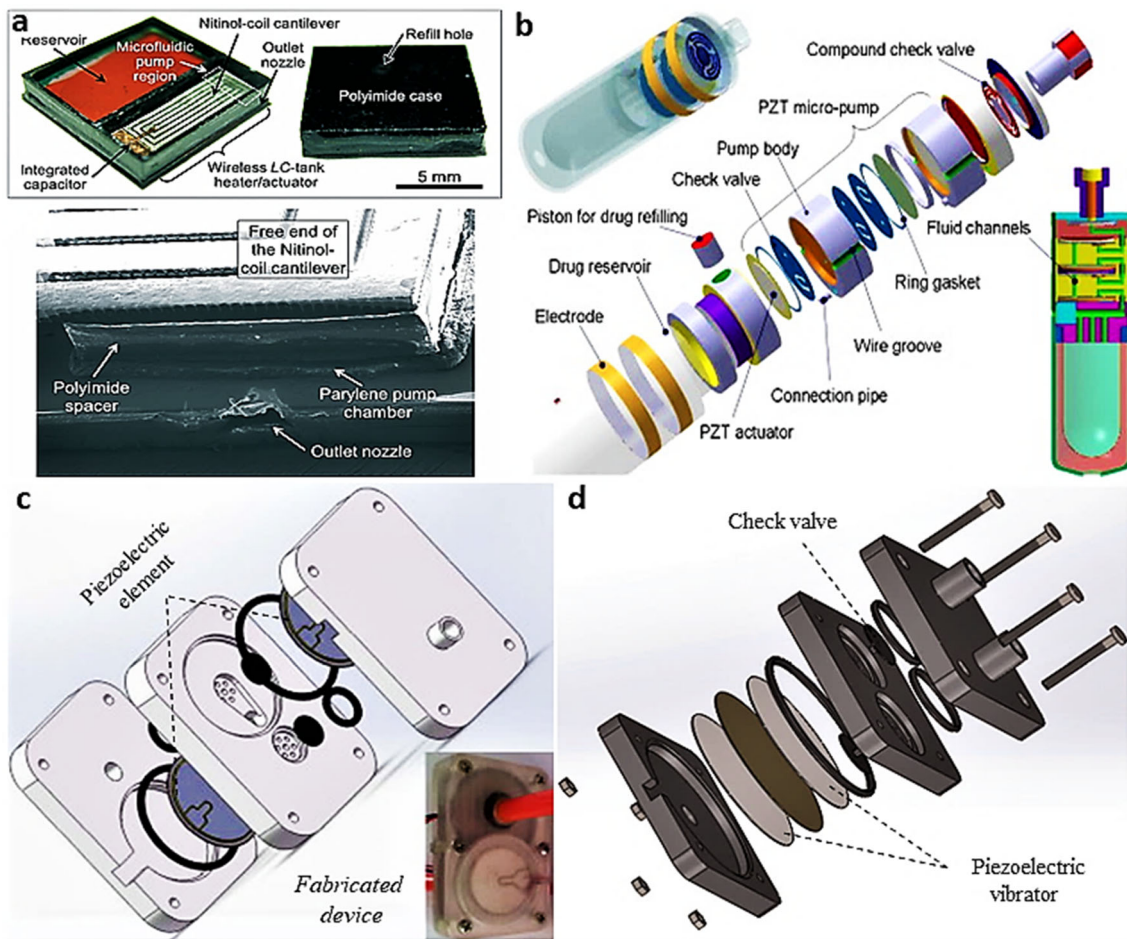
Fig. 12 Micropumps. **a** SMA actuator for drug delivery device. Reproduced with permission from Ref. [210]. Copyright Fong et al. (2015), The Royal Society of Chemistry. **b** Schematic diagram of disposable piezoelectric micropump. Reproduced with permission from Liu et al. (2010), Elsevier. **c** Dual actuator micropump. Reproduced with permission from Zhang et al. (2013), Elsevier. **d** Dual actuator micropump with bimorph transducer. Reproduced with permission from Zhang et al. (2016), SAGE Publications

and a styrene-ethylene butylene styrene impermeable film on top. With an applied liquid pressure, the SMP microvalve transferred working fluid at a flow rate of ~ 250 μL/min. In addition, thermo-responsive hydrogel incorporated microvalves have been utilized frequently in drug delivery devices. Rahimi et al. developed a wirelessly controlled drug delivery device for implant applications that employ RF magnetic fields (Rahimi et al. 2011). The microvalves that operated the device's drug reservoir was made from poly(N-isopropyl acrylamide) hydrogel, which actuated by the activated wireless resonant heater once the field frequency was tuned to the heater circuit's resonance frequency. The device flow rates, and drug release kinetics can also be controlled wirelessly. For example, Nafea et al. (2018) fabricated a magnetic field enabled wirelessly controlled piezoelectric microvalve, as shown in Fig. 13b.

The magnetic field excited the LC resonant circuit, causing a pressure difference in the reservoir to release the stored fluid. At a maximum input pressure, they achieved maximum flow rates of 8.91 and 7.42 m/min in air and phosphate buffered saline solution, respectively. Despite the advantages, the majority of the actuators mentioned above have low displacements. Magnetic actuators outperform thermo-responsive and piezoelectric actuators in terms of high response times and large displacement volumes. For instance, on a programmable microfluidics platform, Pradeep et al. (2018) reported electromagnetically actuated valves that regulated multiple fluids (Fig. 13c). The valves comprised of steel pieces glued to a PDMS membrane, and a series of solenoids to regulate their deflection of up to 120 mm.

3.2 Surgical and endoscopic devices

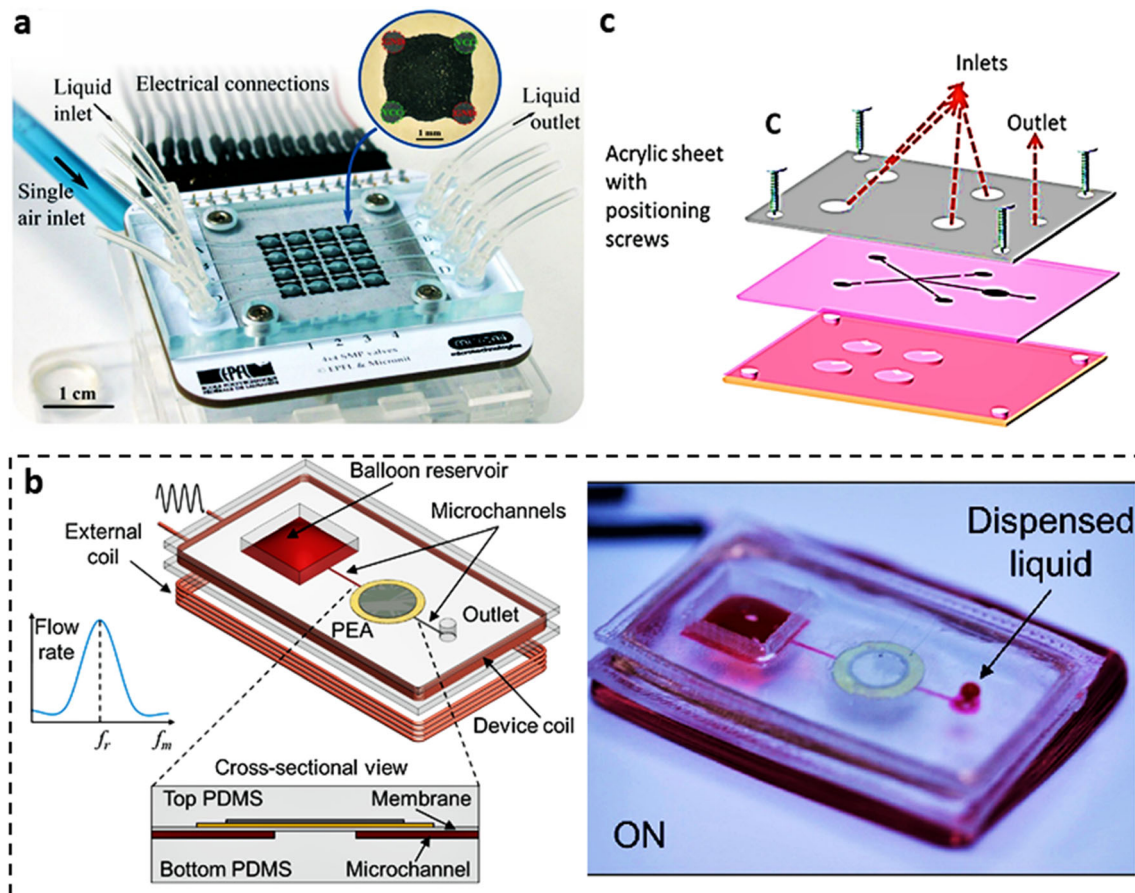Without a doubt, surgical and endoscopic devices are essential tools very much needed for surgical conduct. In

Fig. 13 a SMP-based microfluidic valve. Reproduced with permission from Aksoy et al. (2019), Elsevier. **b** Piezoelectric microvalve. Reproduced with permission from Nafea et al. (2018), Elsevier.

c Schematic diagram of microfluidic channel with active valves. Reproduced with permission from Pradeep et al. (2018), Elsevier

view of the further miniaturization of devices and the increase in complexity of MEMS actuators, they offer promising opportunities for creating novel surgical devices for a broad range of bioMEMS applications. For example, microsurgery assembly (Shi et al. 2014), catheters (Oxley et al. 2016), and selective manipulation (Pan et al. 2017) of cells are based on thermo-responsive materials, piezoelectric, magnetic and soft actuation principles. These actuators can improve the tools for surgical and related procedures, including catheters, endoscopes, and manipulators for grasping and manipulating small or micro-objects. SMA microactuators have been widely used to drive catheters and endoscope tools in various directions, utilizing biocompatibility and superelastic behavior (Chang et al. 2002). For instance, Abadie et al. (2009) developed a comprehensive thermoelectric SMA micro-actuator for active endoscopy that was made up of SMA coils that can bend, twist, and linearly elongate upon heating (Haga et al. 2000; Namazu et al. 2011).

However, issues such as inadequate stroke, slow motion, and unfavorable heat generation must be resolved.

Adldoost et al. (2012) designed a surgical gripper with a single SMA braided wire in a spiral sheath. In addition, Jang et al. developed a teleoperated surgical robot with two end-effectors controlled by SMA, with the goal of implementing compact and lightweight devices capable of driving hand-operated commercial surgical tools such as forceps and scissors (Jang et al. 2020). A pair of SMA wires regulated the forceps, and an SMA spring provided a sustained and stable clamping force (Yuan et al. 2014). An SMA driven compact robotic was also developed to perform single incision laparoscopic surgery (Ali and Takahata 2010; Shi et al. 2014). Magnetic actuators are standard actuators used in capsule endoscopy to image the areas of the small intestine unreachable by traditional endoscopy procedures. A magnetic field-controlled capsule contained a wireless camera, light sources, and a transmitter. After being ingested by the patient, it took pictures of the digestive tract and transmitted them to a recorder worn by the patient ("Capsule Endoscopy—All medical specialities—Olympus Medical Systems, Europe," 2019). Olympus® developed a magnetically actuated capsule endoscope

that featured an internal permanent magnet and a spiral ridge wrapped around the capsule body which could be driven forward and backwards when an external rotating magnet was applied (Moglia et al. 2007; Toennies et al. 2010). Garbin et al. (2015) developed a laparoscopic tissue retractor with an actuation unit consisting of an external driving unit (EDM), an internal driven magnet (IDM), and a pair of internal anchoring magnets and external permanent anchoring magnets using local magnetic actuation. Meanwhile, Di Natali et al. (2015) reported a manipulator with three pairs of EDMs and IDMs and an anchoring unit to execute surgical tasks (Fig. 14a). Aside from local magnetic actuation, several researchers have reported ferromagnetic-body-based magnetic actuators driven by MRI gradients. One notable work is reported by Vartholomeos et al., where an MRI-powered actuator was developed for needle insertion in neurosurgery. It had a mechanism capable of converting the rotational motion of spherical ferromagnetic particles into linear motion to operate a non-magnetic biopsy needle (Vartholomeos et al. 2011).

Aside from magnetic-based actuation approaches, attempts have been made to develop various surgical instruments using pneumatic and other fluid-driven actuators. For example, several pairs of PBA were reported to generate telescopic motion by manipulating force for

commercial forceps (Fujiwara et al. 2009). Ruzzu et al. (1998) devised a three-inflatable micro-balloon device for positioning and orienting the catheter tip. These micro-balloons were attached to the catheter tip on three sides and operated by electro-thermo-pneumatic micro-valves. Researchers have adapted soft PSA for specific biomedical applications in addition to PBAs in medical instruments and systems. For example, Ranzani et al. (2015) developed a surgical manipulator inspired by an octopus tentacle, consisting of two identical modules with multi-directional bending and stiffening capabilities. In a previous study, Surakusumah et al. (2014), to observe the lungs, airway, and bronchus obstructions, researchers developed a PSA-based flexible bronchoscope (FOB) that provided displacement through twisting and bending motions (Fig. 14b). Furthermore, a pneumatically actuated micro-gripper was reported by Alogla et al. (2015) to manipulate embryos for cloning applications. The micro-gripper consisted of two main components, namely, a micro pneumatic chamber with a flexible membrane and hinged gripper arms attached to the membrane deflected to provide gripping motion when pressurized air was supplied to the membrane as shown in Fig. 14c. Traditional laparoscopes used for some surgical procedures (such as complete mesorectal excision) lack the versatility needed to maneuver and meet
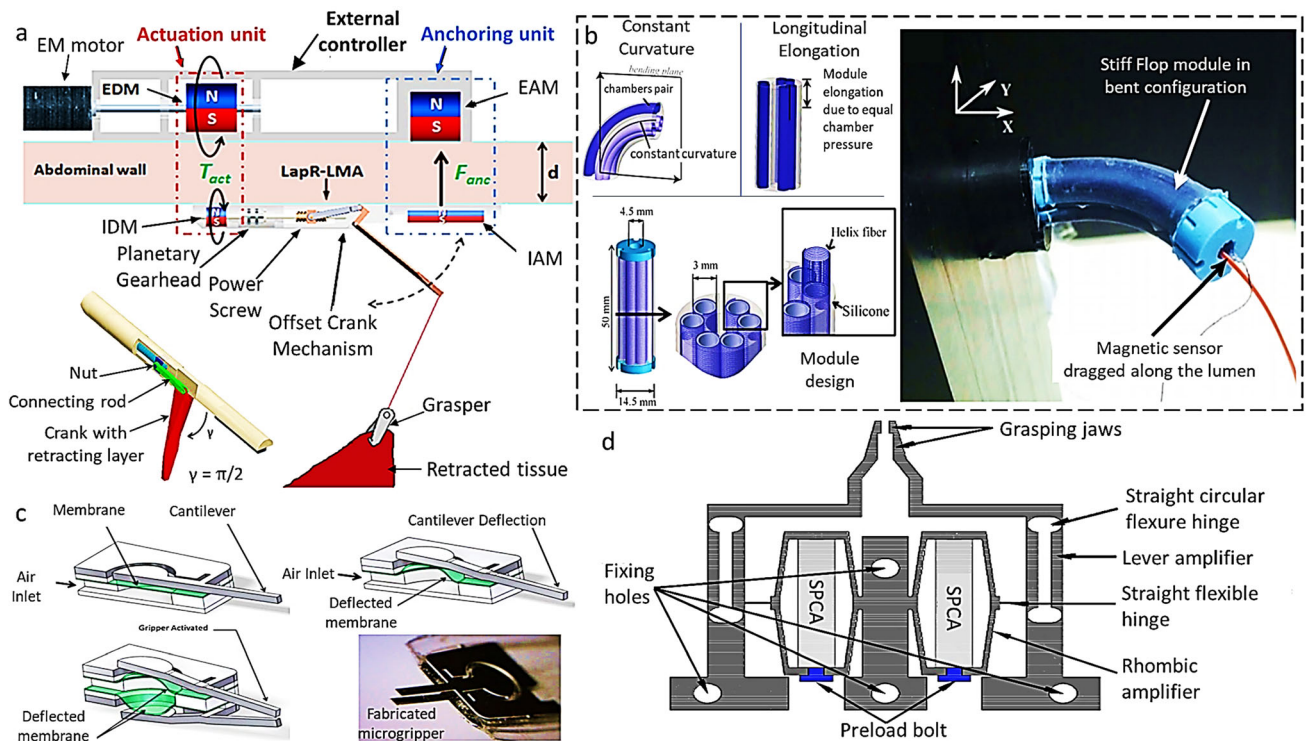

Fig. 14 **a** Magnetic actuated endoscopy. Reproduced with permission from Di Natali et al. (2015), Wiley. **b** Pneumatic flexible bronchoscope. Reproduced with permission from Surakusumah et al. (2014), IEEE. **c** Pneumatic microgripper. Reproduced with permission from

Alogla et al. (2015), Elsevier. **d** Piezoelectric actuated microgripper. Reproduced with permission from Chen et al. (2019a), Nanotechnology and Precision Engineering)
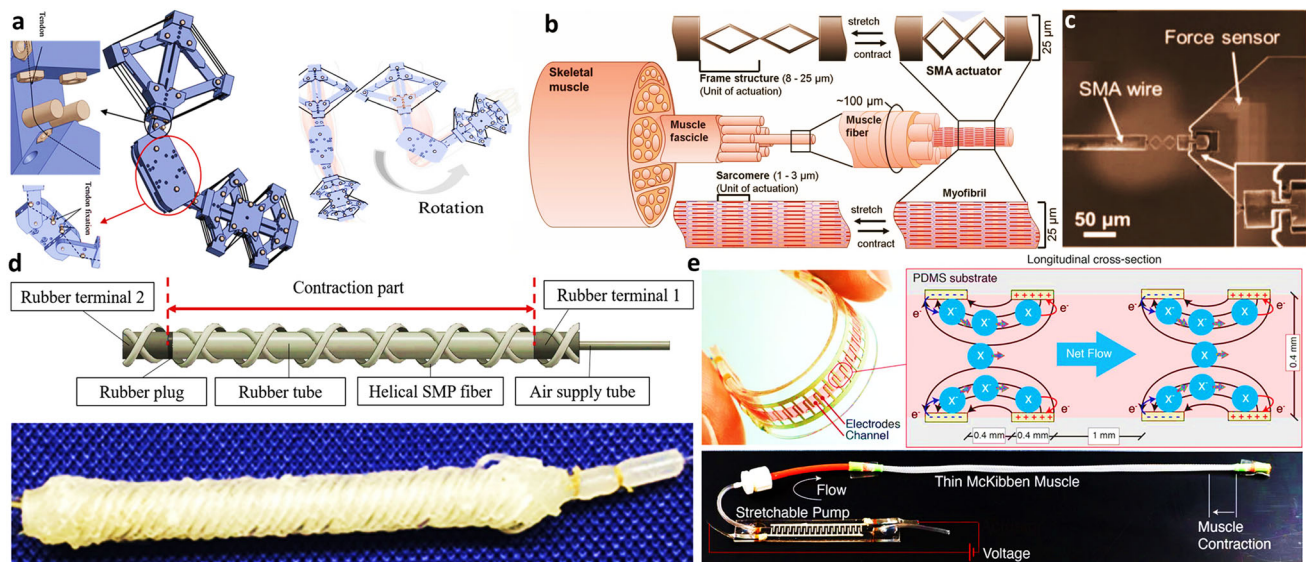
Fig. 15 a SMA actuator artificial muscle for robotic elbow joint. Reproduced with permission from Park et al. (2020), Elsevier. SMA-based microscale actuator. b Schematic diagram and its c SEM image. Reproduced with permission from Lee et al. (2018), Wiley–VCH. d Schematic design (above) and fabricated image (below) of the helical SMP fibers. Reproduced with permission from Yahara et al. (2019), Elsevier. e Schematic design (above) and fabricated image (below) of the McKibben Muscles. Reproduced with permission from Cacucciolo et al. (2019), Frontiers

complex surgical targets safely. Thus, Abidi et al. (2018) and Diodato et al. (2018) designed a robotic system of two pneumatically actuated identical modules capable of multi-directional bending and elongation, allowing for highly dexterous and secure navigation.

Precision positioning and micromanipulation of tiny objects are of great interest in tissue engineering and minimally invasive surgery. Thus, microgrippers have been developed for grabbing, holding, and delivering micro-objects to a specific position. The actuator is an essential part of the microgripper; it provides the necessary force to make the device function as a gripper (Nah and Zhong 2007). Even though various actuators have been used in microgrippers, piezoelectric actuators have been the most popular due to their advantages, such as fast response times and high displacement accuracy. Piezoelectrically actuated microgrippers have considerably satisfied the requirements for grabbing tiny objects with improved accuracy and high-resolution capabilities. For instance, Chen et al. (2019a, b; 2020) designed and developed a piezoelectric-actuated microgripper consisting of flexible hinges, grasping jaw, and amplifiers shown in Fig. 14d. The gripper was capable of holding any objects of size within the range of 0–1724 μm. In addition, Das et al. (2020) developed a flexure-based piezoelectric microgripper that demonstrated the task of grabbing and releasing micro-wire with a total output displacement of 338.3 μm. A piezoelectric actuated microgripper with a three-stage micromanipulation amplification mechanism was designed and developed by Liang et al. (2018) that provided a displacement of 20 μm.

3.3 Artificial muscle

Artificial muscle, also known as muscle-like actuators, is a broad term for a class of materials that can mimic natural muscle movement. Similar to natural muscle, artificial muscle is defined by its ability to contract in response to a chemical or physical stimulus. They can change their stiffness, contract, expand, or rotate within one component in response to an external stimulus such as voltage, current, pressure, light, or temperature (Mirvakili and Hunter 2018). Skeletal muscle contraction is essentially a straight contraction. Meanwhile, the term "artificial muscle contraction" has a broader meaning: it can refer to the straight contraction of a complex structure in the case of fluidic artificial muscles with a sheath, or the straight contraction of a thin string in the case of shape-memory materials, such as nitinol filaments. In general, any substance or device whose shape can change in response to a stimulus may be considered an "artificial muscle".

Low-power mobile actuators, robots that replicate efficient and natural forms of motion, autonomous robots and sensors, and lightweight wearable technology are possible with today's artificial muscle technology. However, it is still unclear which material has the ability to form the optimal artificial muscle. Some of the studied artificial muscles used SMA, SMP, pneumatic, DE, and HASEL. The advantages of SMA artificial muscle are their lightness and high energy density. The high energy density allows the actuator to generate powerful motions. Park et al. (2020) developed the use of SMA wire as an actuation
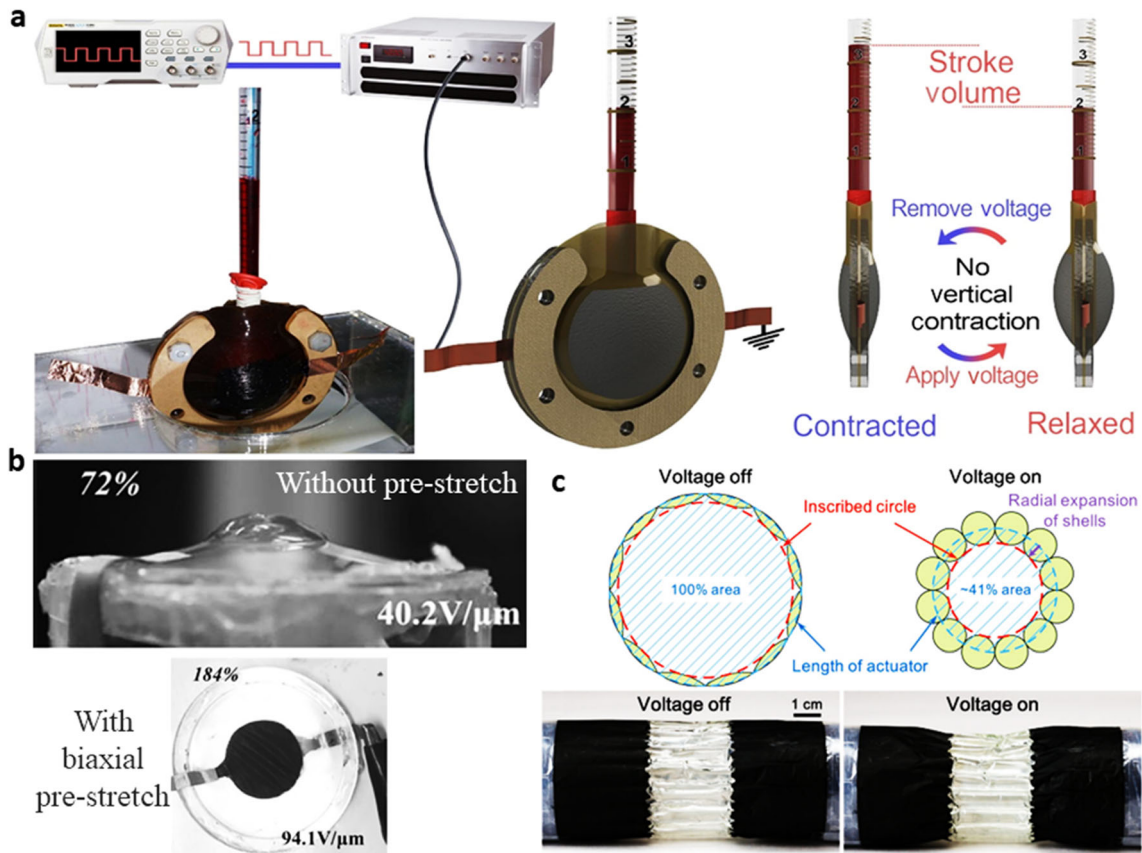
Fig. 16 a DEA for soft artificial heart. Reproduced with permission from Wu et al. (2021), Elsevier. **b** DEA with *pentablock copolymer*. Reproduced with permission from Chen et al. (2021), Elsevier. **c** Actuation of HS Peano-HASEL (above) and cylindrically pump high strain Peano-HASEL actuator (below). Reproduced with permission from Wang et al. (2020), Wiley–VCH

material for prosthetic muscle elbow joints (Fig. 15a). The elbow joint produced a maximum force of 56.3 N and had response times of 3–5 s for lifting and 8–12 s for lying down. Meanwhile, Lee et al. (2012) developed a new prosthetic hand driving mechanism with a fixed thumb and four fingers powered by an artificial muscle of the SMA type. SMA-based microscale actuators were also fabricated by Lee et al. (2018) using diamond-shaped frame components. Compared to bulk SMA materials, such structures allow for a wide elongation range due to spring-like behavior during tensile deformation. However, most SMA artificial muscles are inflexible (Fig. 15bc). Alternatively, Taniguchi (2013) proposed a flexible artificial muscle actuator based on the molding of silicone rubber utilizing coiled SMA wires. Apart from SMA, numerous attempts have been made to modify SMP in artificial muscle because they have high strains, are flexible at high temperatures, and the simplicity of manufacturing complex 3D structures. For instance, Fan and Li (2017) made chemically cross-linked poly(ethylene-*co*-vinyl acetate) two-way SMP precursor fibers. Artificial muscles were created by twisting precursor fibers and displayed an actuation strain

of up to 68% in the muscle. In artificial muscle made by Yahara et al. (2019), helical SMP fibers were used as sleeve fibers. The helical SMP fibers' sleeve angles could be altered following fabrication procedures due to their shape fixity (Fig. 15d).

Other than SMA and SMP artificial muscle, pneumatic actuators are among the most frequently use in artificial muscle application. McKibben actuators or pneumatic artificial muscles have been designed using appropriate silicone rubbers containing a type of fluid, such as air, to supply energetic sources for the expansion and contraction of the allegedly artificial muscle. For example, Yang et al. (2019) demonstrated a high displacement pneumatic artificial muscle made of textiles with integrated electronics to sense its pressure and displacement, attaining a high contraction ratio of 40–65%. Cacucciolo et al. (2019) described an electrically-driven soft fluidic muscle combining thin fiber-like McKibben actuators with fully stretchable pumps. The pumps relied on a solid-state pumping mechanism (electrohydrodynamics), which used an electric field to directly accelerate liquid molecules through an electric field (Fig. 15e).

Table 5 Summary of actuation techniques

Types		Material	Advantages	Disadvantages	MEMS biomedical application
Thermo-responsive actuator	SMA	Ni–Ti alloy, Fe–Mn-SI, Cu–Zn-Al, Cu-Al-Ni	Large displacement Large force High mechanical robustness Corrosion resistant	Slow temporal response High power consumption	Medical and surgical tools
	SMP	Polyethylene, polyurethane, PLA	Structural flexibility Large strain Low density Biodegradable properties	Slow temporal response Low recovery stress	Drug delivery devices
Piezoelectric actuator		Lead zirconate titanate (PZT), barium titanate, lead titanate, lithium niobate, lithium tantalite	High displacement resolution Fast response time High efficiency	High driving voltage Require high temperature to process piezo material	Micropumps, microgrippers
Magnetic actuator		NdFeB	Large deflection at low voltage High field energy density Fast response time Simple drive mode	High power dissipation for driving coils	Microgripper, micropumps, microvalves
Soft actuator	Pneumatic	PDMS, Ecoflex 0030, silicon rubber	High flexibility Large displacement High power to weight ratio	Low force exertion Limited number of degrees of freedom	Medical devices
	IPMC	Nafion, Flemion, Aciplex, ionic hydrogel, conducting polymer	High durability Low activation voltage Rapid response Large bending displacement	Slow response time Low electromechanical coupling efficiency	Micropump, surgical tools
	DE	VHB 4910	Mechanical flexibility Low density Simple fabrication process	Requires high field strength Low viscoelasticity of elastomer	Microgripper, micropump
	HASEL	Ecoflex 0030, BOPP film	Fast response time High displacement Self-sensing ability	High activation voltage	Artificial muscle

Besides, according to Qiu et al. (2019), although DEAs are considered new in the artificial muscle industry, DEAs reflect their high potential as significant technological progress has shown due to the mechanisms designed to utilize their large-strain actuation and low stiffness. Qin et al. (2018) created soft planar DEA artificial muscles for jaw movement and vibration shaker in tactile feedback with a maximum linear strain of more than 90%. The fabricated DEA employed a compression spring for free-standing structure, achieving linear actuation and twisting without the actuator's size increment. Other than that, a new dipole-conformation-actuated strain cross-scale model to explain the actuated strain of DE was proposed by Wu et al. (2021), and a new DE based on polyphosphazene was synthesized. As a result, a soft artificial heart based on polyphosphazene was built and showed great potential for heart failure patients (Fig. 16a). However, DEA artificial muscle generally requires a very high actuation voltage and lowering it to less than 1 kV remains a great challenge. Thus, Chen et al. (2021) reported a pentablock copolymer (SEHAS: S for polystyrene, EHA for poly(2-ethylhexyl acrylate)) with a low actuation voltage and an ultrasoft-yet-strong property (Fig. 16b). Furthermore, HASEL actuators have demonstrated good potential as an artificial muscle. They rely on a BOPP film material that tenses up once a voltage is applied, as presented in Fig. 16c. They represent a breakthrough in soft robotics because these actuators are the closest replication to a human muscle. These actuators can withstand a strain of 0.3 MPa, similar to that of a human arm muscle. By wrapping a 12-unit HS-Peano HASEL actuator around a silicone tube, Wang et al. (2020) fabricated a bioinspired artificial circular muscle (ACM) that acted as a pump.

4 Conclusion and future prospects

The performance and versatility of MEMS-actuators, as well as their fabrication and integration methods, have shown tremendous advancements. They have contributed to the emerging field of biomedical microsystems such as smart implants and miniaturized surgical devices. Table 5 compares these actuation mechanisms and their properties in detail. The success of a targeted application is heavily reliant on proper actuator selection, which is determined by factors other than the actuator's fundamental efficiency, such as powering and control methods, biocompatibility, and cost effectiveness. It is essential to have a suitable actuation mechanism driving a medical system, as any malfunction in the system during medical or surgical procedures can be fatal. As a result, a comprehensive analysis of appropriate and widely used actuation methods such as SMA, SMP, magnetic, piezoelectric, DE, IPMC, pneumatic, and HASEL on their applications in biomedical devices is carried out.

While most of the reported works remained in the research phase, a few have reached the commercialization phase. Thermo-responsive actuators, i.e., SMA and SMP, are feasible for driving medical tools, equipment, and implantable devices. While magnetic actuation is feasible for attaining 360° rotation motion especially in capsule endoscopy applications. Based on the reviewed literature, Table 5 presents a summarized comparison of various actuation techniques and their applications. It can be concluded that all the actuation mechanisms reported here show considerable potential. However, being soft, safe, and flexible, PSA-based actuation mechanisms can push the boundaries of the biomedical field towards the development of more versatile medical systems in the future. Among them, SMA offers large displacement and force whereas SMP possesses relatively high recoverable strain levels. They are often used in drug delivery and surgical devices owing to their characteristics mentioned above. Electromagnetic actuators are used to develop micropumps and microvalves because of their large displacement, fast reaction, and low-voltage powering. Meanwhile, piezoelectric actuators are an established technology for devices aimed at micro-scale positioning and micropumps. Being softer and flexible, pneumatic, IPMC, and DE actuators offer a variety of application opportunities in surgical devices. However, there still remain certain inherent challenges in these actuators, such as limited number of degrees of freedom, slow response times, and low force exertion. Consequently, the newly developed HASEL actuator is a great substitute as it provides a large displacement and fast response time suitable for the development of artificial muscle.

Based on the literature review, most actuation field research focuses on soft actuators for biomedical applications. MEMS technology and microfabrication advances have enabled soft actuators to generate adequate displacement for biomedical devices. The development of hybrid actuators, which combine DEA and fluid-driven soft actuators to address the limitations of DEA, is seen as a promising approach to improve displacement output. In conclusion, the ongoing advancements in soft actuation techniques, characterized by reduced power requirements and compatibility with biomedical devices, will provide a sustainable platform for future diagnostic and therapeutic applications.

References

Abadie J, Chaillet N, Lexcellent C (2009) Modeling of a new SMA micro-actuator for active endoscopy applications. Mechatronics 19(4):437–442

Abidi H, Gerboni G, Brancadoro M, Fras J, Diodato A, Cianchetti M, Menciassi A et al (2018) Highly dexterous 2-module soft robot for intra-organ navigation in minimally invasive surgery. Int J Med Robot Comput Assist Surg 14(1):e1875

AbuZaiter A, Ali MSM (2014) Analysis of thermomechanical behavior of shape-memory-alloy bimorph microactuator. In: 5th International Conference on Intelligent Systems, Modelling and Simulation, pp 390–393

AbuZaiter A, Ng EL, Kazi S, Mohamed Ali MS (2015a) Development of miniature stewart platform using TiNiCu shape-memory-alloy actuators. Adv Mater Sci Eng 2015

AbuZaiter A, Ng EL, Ali MSM, Kazi S (2015b) Miniature parallel manipulator using TiNiCu shape-memory-alloy microactuators. In: 10th Asian Control Conference (ASCC), pp 1–4

AbuZaiter A, Nafea M, Ali MSM (2016a) Development of a shape-memory-alloy micromanipulator based on integrated bimorph microactuators. Mechatronics 38:16–28

AbuZaiter A, Nafea M, Mohd Faudzi AA, Kazi S, Mohamed Ali MS (2016b) Thermomechanical behavior of bulk NiTi shape-memory-alloy microactuators based on bimorph actuation. Microsyst Technol 22:2125–2131

Acome E, Mitchell S, Morrissey T, Emmett M, Benjamin C, King M, Keplinger C et al (2018) Hydraulically amplified self-healing electrostatic actuators with muscle-like performance. Science 359(6371):61–65

Adldoost H, Jouibary BR, Zabihollah A (2012) Design of SMA micro-gripper for minimally invasive surgery. In: IEEE 19th Iranian conference of Biomedical Engineering (ICBME), pp 97–100

Agarwal G, Besuchet N, Audergon B, Paik J (2016) Stretchable materials for robust soft actuators towards assistive wearable devices. Sci Rep 6(1):1–8

Ajili SH, Ebrahimi NG, Soleimani M (2009) Polyurethane/poly-caprolactane blend with shape memory effect as a proposed material for cardiovascular implants. Acta Biomater 5(5):1519–1530

Aksoy B, Besse N, Boom RJ, Hoogenberg B-J, Blom M, Shea H (2019) Latchable microfluidic valve arrays based on shape memory polymer actuators. Lab Chip 19(4):608–617

Algamili AS, Khir MHM, Dennis JO, Ahmed AY, Alabsi SS, Hashwan SSB, Junaid MM (2021) A review of actuation and sensing mechanisms in mems-based sensor devices. Nanoscale Res Lett 16(1):1–21

Ali MSM, Takahata K (2010) Frequency-controlled wireless shape-memory-alloy microactuators integrated using an electroplating bonding process. Sens Actuators A 163(1):363–372

Ali MSM, Bycraft B, Bsoul A, Takahata K (2012) Radio-controlled microactuator based on shape-memory-alloy spiral-coil inductor. J Microelectromech Syst 22(2):331–338

Alogla A, Amalou F, Balmer C, Scanlan P, Shu W, Reuben R (2015) Micro-tweezers: design, fabrication, simulation and testing of a pneumatically actuated micro-gripper for micromanipulation and microtactile sensing. Sens Actuators A 236:394–404

Amirouche F, Zhou Y, Johnson T (2009) Current micropump technologies and their biomedical applications. Microsyst Technol 15(5):647–666

Anderson IA, Gisby TA, McKay TG, O'Brien BM, Calius EP (2012) Multi-functional dielectric elastomer artificial muscles for soft and smart machines. J Appl Phys 112(4):041101

Araromi OA, Gavrilovich I, Shintake J, Rosset S, Richard M, Gass V, Shea HR (2014) Rollable multisegment dielectric elastomer minimum energy structures for a deployable microsatellite gripper. IEEE/ASME Trans Mechatron 20(1):438–446

Ariano P, Accardo D, Lombardi M, Bocchini S, Draghi L, De Nardo L, Fino P (2015) Polymeric materials as artificial muscles: an overview. J Appl Biomat Funct Mater 13(1):1–9

Ashley S (2003) Artificial muscles. Sci Am 289(4):52–59

Ayvali E, Desai JP (2012) Motion planning for the discretely actuated steerable cannula. In: IEEE 4th RAS & EMBS International Conference on Biomedical Robotics and Biomechatronics (BioRob), pp 50–55

Bar-Cohen Y, Anderson IA (2019) Electroactive polymer (EAP) actuators—background review. Mech Soft Mater 1(1):5

Baù M, Ferrari V, Marioli D, Sardini E, Serpelloni M, Taroni A (2008) Contactless electromagnetic excitation of resonant sensors made of conductive miniaturized structures. Sens Actuators A 148(1):44–50

Bau M, Ferrari V, Maroli D (2009) Contactless excitation of MEMS resonant sensors by electromagnetic driving. In: Proceedings of the COMSOL Conference.

Beasley RA (2012) Medical robots: current systems and research directions. J Robot 2012

Belding L, Baytekin B, Baytekin HT, Rothemund P, Verma MS, Nemiroski A, Whitesides GM et al (2018) Slit tubes for semisoft pneumatic actuators. Adv Mater 30(9):1704446

Benard WL, Kahn H, Heuer AH, Huff MA (1998) Thin-film shape-memory alloy actuated micropumps. J Microelectromech Syst 7(2):245–251

Besse N, Rosset S, Zarate JJ, Ferrari E, Brayda L, Shea H (2017a) Understanding graphics on a scalable latching assistive haptic display using a shape memory polymer membrane. IEEE Trans Haptics 11(1):30–38

Besse N, Rosset S, Zarate JJ, Shea H (2017b) Flexible active skin: large reconfigurable arrays of individually addressed shape memory polymer actuators. Adv Mater Technol 2(10):1700102

Bigué J-PL, Plante J-S (2011) Experimental study of dielectric elastomer actuator energy conversion efficiency. IEEE/ASME Trans Mechatron 18(1):169–177

Brochu P, Pei Q (2012) Dielectric elastomers for actuators and artificial muscles. In: Electroactivity in polymeric materials, pp 1–56

Byrne O, Coulter F, Glynn M, Jones JF, Ní Annaidh A, O'Cearbhaill ED, Holland DP (2018) Additive manufacture of composite soft pneumatic actuators. Soft Robot 5(6):726–736

Cacucciolo V, Nabae H, Suzumori K, Shea H (2019) Electrically-driven soft fluidic actuators combining stretchable pumps with thin McKibben muscles. Front Robot AI 6:146

Capsule Endoscopy (2019) All medical specialities—Olympus Medical Systems, Europe

Ceyssens F, Sadeghpour S, Fujita H, Puers R (2019) Actuators: accomplishments, opportunities and challenges. Sens Actuators A 295:604–611

Chang JK, Chung S, Lee Y, Park J, Lee S-K, Yang SS, Han D-C et al (2002) Development of endovascular microtools. J Micromech Microeng 12(6):824

Chang XL, Chee PS, Lim EH (2018) A Microreservior-based drug delivery device using ionic polymer metal composite (IPMC) actuator. In: TENCON 2018-2018 IEEE Region 10 Conference IEEE, pp 0899–0902

Chang XL, Chee PS, Lim EH, Chong WC (2018b) Radio-frequency enabled ionic polymer metal composite (IPMC) actuator for drug release application. Smart Mater Struct 28(1):015024

Chen X, Su C-Y, Li Z, Yang F (2016) Design of implementable adaptive control for micro/nano positioning system driven by

piezoelectric actuator. IEEE Trans Ind Electron 63(10):6471–6481

Chen T, Bilal OR, Lang R, Daraio C, Shea K (2019a) Autonomous deployment of a solar panel using elastic origami and distributed shape-memory-polymer actuators. Phys Rev Appl 11(6):064069

Chen X, Deng Z, Hu S, Gao J, Gao X (2019b) Design of a flexible piezoelectric microgripper based on combined amplification principles. Nanotechnol Precis Eng 2(3):138–143

Chen X, Deng Z, Hu S, Gao J, Gao X (2020) Designing a novel model of 2-DOF large displacement with a stepwise piezoelectric-actuated microgripper. Microsyst Technol 26(9):2809–2816

Chen Z, Xiao Y, Fang J, He J, Gao Y, Zhao J, Luo Y et al (2021) Ultrasoft-yet-strong pentablock copolymer as dielectric elastomer highly responsive to low voltages. Chem Eng J 405:126634

Choudhary N, Kaur D (2016) Shape memory alloy thin films and heterostructures for MEMS applications: a review. Sens Actuators A 242:162–181

Cobo A, Sheybani R, Meng E (2015) MEMS: enabled drug delivery systems. Adv Healthc Mater 4(7):969–982

Das TK, Shirinzadeh B, Al-Jodah A, Ghafarian M, Pinskier J (2020) Computational parametric analysis and experimental investigations of a compact flexure-based microgripper. Precis Eng 66:363–373

de Saint-Aubin C, Rosset S, Schlatter S, Shea H (2018) High-cycle electromechanical aging of dielectric elastomer actuators with carbon-based electrodes. Smart Mater Struct 27(7):074002

De Volder M, Reynaerts D (2010) Pneumatic and hydraulic microactuators: a review. J Micromech Microeng 20(4):043001

Di Natali C, Mohammadi A, Oetomo D, Valdastri P (2015) Surgical robotic manipulator based on local magnetic actuation. J Med Devices 9(3)

Digumarti KM, Conn AT, Rossiter J (2017) Euglenoid-inspired giant shape change for highly deformable soft robots. IEEE Robot Autom Lett 2(4):2302–2307

Ding Z, Dong J, Yin H, Wang Z, Zhou X, Xu Z (2019) Design and experimental performances of a piezoelectric stick-slip actuator for rotary motion. In: IOP Conference Series: Materials Science and Engineering, vol 563, No 4, p 042068

Diodato A, Brancadoro M, De Rossi G, Abidi H, Dall'Alba D, Muradore R, Cianchetti M et al (2018) Soft robotic manipulator for improving dexterity in minimally invasive surgery. Surg Innov 25(1):69–76

Fan J, Li G (2017) High performance and tunable artificial muscle based on two-way shape memory polymer. RSC Adv 7(2):1127–1136

Fong J, Xiao Z, Takahata K (2015) Wireless implantable chip with integrated nitinol-based pump for radio-controlled local drug delivery. Lab Chip 15(4):1050–1058

Forbrigger C, Lim A, Onaizah O, Salmanipour S, Looi T, Drake J, Diller ED (2019) Cable-less, magnetically driven forceps for minimally invasive surgery. IEEE Robot Autom Lett 4(2):1202–1207

Fujiwara N, Sawano S, Konishi S (2009) Linear expansion and contraction of paired pneumatic baloon bending actuators toward telescopic motion. In: IEEE 22nd International Conference on Micro Electro Mechanical Systems. pp 435–438

Gao X, Yang J, Wu J, Xin X, Li Z, Yuan X, Dong S et al (2020) Piezoelectric actuators and motors: materials, designs, and applications. Adv Mater Technol 5(1):1900716

Garbin N, Di Natali C, Buzzi J, De Momi E, Valdastri P (2015) Laparoscopic tissue retractor based on local magnetic actuation. J Med Devices 9(1)

Ge Q, Sakhaei AH, Lee H, Dunn CK, Fang NX, Dunn ML (2016) Multimaterial 4D printing with tailorable shape memory polymers. Sci Rep 6:31110

Ge L, Wang T, Zhang N, Gu G (2018) Fabrication of soft pneumatic network actuators with oblique chambers. J Vis Exp JoVE (138)

Ghazali FAM, Mah CK, AbuZaiter A, Chee PS, Ali MSM (2017) Soft dielectric elastomer actuator micropump. Sens Actuators A 263:276–284

Ghazali FAM, Hasan MN, Rehman T, Nafea M, Ali MSM, Takahata K (2020) MEMS actuators for biomedical applications: a review. J Micromech Microeng 30(7):073001

Gidde RR, Pawar PM, Ronge BP, Dhamgaye VP (2019) Design optimization of an electromagnetic actuation based valveless micropump for drug delivery application. Microsyst Technol 25(2):509–519

Gifari MW, Naghibi H, Stramigioli S, Abayazid M (2019) A review on recent advances in soft surgical robots for endoscopic applications. Int J Med Robot Comput Assist Surg 15(5):e2010

Gomis-Bellmunt O, Campanile LF (2009) Design rules for actuators in active mechanical systems. Springer Science & Business Media.

Gorissen B, Chishiro T, Shimomura S, Reynaerts D, De Volder M, Konishi S (2014) Flexible pneumatic twisting actuators and their application to tilting micromirrors. Sens Actuators A 216:426–431

Gorissen B, De Volder M, Reynaerts D (2018) Chip-on-tip endoscope incorporating a soft robotic pneumatic bending microactuator. Biomed Microdevice 20(3):1–7

Gunda A, Özkayar G, Tichem M, Ghatkesar MK (2020) Proportional microvalve using a unimorph piezoelectric microactuator. Micromachines 11(2):130

Guo J, Sun Y, Liang X, Low JH, Wong YR, Tay VSC, Yeow CH (2017) Design and fabrication of a pneumatic soft robotic gripper for delicate surgical manipulation. In: IEEE International Conference on Mechatronics and Automation (ICMA), pp 1069–1074

Gu-Stoppel S, Timmermann M, Lisec T, Lofink F (2019) Magnetically Driven Actuators for Vector Scanning Mems Mirrors. In: 20th International Conference on Solid-State Sensors, Actuators and Microsystems & Eurosensors XXXIII (TRANSDUCERS & EUROSENSORS XXXIII), pp 1507–1510

Haga Y, Esashi M, Maeda S (2000) Bending, torsional and extending active catheter assembled using electroplating. In: Proceedings IEEE 13th Annual International Conference on Micro Electro Mechanical Systems (Cat. No. 00CH36308), pp 181–186

Hamid NA, Majlis BY, Yunas J, Syafeeza A, Wong YC, Ibrahim M (2017) A stack bonded thermo-pneumatic micro-pump utilizing polyimide based actuator membrane for biomedical applications. Microsyst Technol 23(9):4037–4043

Han M-W, Rodrigue H, Cho S, Song S-H, Wang W, Chu W-S, Ahn S-H (2016) Woven type smart soft composite for soft morphing car spoiler. Compos B Eng 86:285–298

Hao M, Wang Y, Zhu Z, He Q, Zhu D, Luo M (2019) A compact review of IPMC as soft actuator and sensor: current trends, challenges, and potential solutions from our recent work. Front Robot AI 6:129

Hasan SM, Nash LD, Maitland DJ (2016) Porous shape memory polymers: Design and applications. J Polym Sci Part B Polym Phys 54(14):1300–1318

He L, Zhao D, Li W, Xu Q, Cheng G (2019) Performance analysis of valveless piezoelectric pump with dome composite structures. Rev Sci Instrum 90(6):065002

Heng KR, Ahmed AS, Shrestha M, Lau GK (2017) Strong dielectric-elastomer grippers with tension arch flexures. In: Electroactive Polymer Actuators and Devices (EAPAD), vol 10163, pp 336–343

Hill M, Rizzello G, Seelecke S (2017) Development of a fatigue testing setup for dielectric elastomer membrane actuators. In:

Electroactive Polymer Actuators and Devices (EAPAD), vol 10163, pp 144–150

Hilt JZ, Peppas NA (2005) Microfabricated drug delivery devices. Int J Pharm 306(1–2):15–23

Holman H, Kavarana MN, Rajab TK (2021) Smart materials in cardiovascular implants: shape memory alloys and shape memory polymers. Artif Organs 45(5):454–463

Horiuchi T, Sugino T, Asaka K (2017) Elliptical-like cross-section ionic polymer-metal composite actuator for catheter surgery. Sens Actuators A 267:235–241

Imai S, Tsukioka T (2014) A magnetic MEMS actuator using a permanent magnet and magnetic fluid enclosed in a cavity sandwiched by polymer diaphragms. Precis Eng 38(3):548–554

Jain RK, Majumder S, Ghosh B (2015) Design and analysis of piezoelectric actuator for micro gripper. Int J Mech Mater Des 11(3):253–276

Jang N, Ihn YS, Choi N, Gu G, Jeong J, Yang S, Hwang D et al (2020) Compact and lightweight end-effectors to drive hand-operated surgical instruments for robot-assisted microsurgery. IEEE/ASME Trans Mechatron 25(4):1933–1943

Janocha H (2004) Actuators. Springer, Berlin

Jayachandran S, Akash K, Prabu SM, Manikandan M, Muralidharan M, Brolin A, Palani I (2019) Investigations on performance viability of NiTi, NiTiCu, CuAlNi and CuAlNiMn shape memory alloy/Kapton composite thin film for actuator application. Compos B Eng 176:107182

Jia S, Peng J, Bian J, Zhang S, Xu S, Zhang B (2021) Design and fabrication of a MEMS electromagnetic swing-type actuator for optical switch. Micromachines 12(2):221

Jo C, Pugal D, Oh I-K, Kim KJ, Asaka K (2013) Recent advances in ionic polymer–metal composite actuators and their modeling and applications. Prog Polym Sci 38(7):1037–1066

Junwu K, Zhigang Y, Taijiang P, Guangming C, Boda W (2005) Design and test of a high-performance piezoelectric micropump for drug delivery. Sens Actuators A 121(1):156–161

Kabla M, Ben-David E, Shilo D (2016) A novel shape memory alloy microactuator for large in-plane strokes and forces. Smart Mater Struct 25(7):075020

Kadir MRA, Dewi DEO, Jamaludin MN, Nafea M, Ali MSM (2019) A multi-segmented shape memory alloy-based actuator system for endoscopic applications. Sens Actuators A 296:92–100

Kalyonov VE, Orekhov YD, Shahabdin AN, Broyko AP, Testov DO (2020) Valveless microfluidic pump based on IPMC actuator for drug delivery. In: IEEE Conference of Russian Young Researchers in Electrical and Electronic Engineering (EIConRus), pp 1531–1534

Kellaris N, Gopaluni Venkata V, Smith GM, Mitchell SK, Keplinger C (2018) Peano-HASEL actuators: muscle-mimetic, electrohydraulic transducers that linearly contract on activation. Sci Robot 3(14):eaar3276

Keplinger C, Li T, Baumgartner R, Suo Z, Bauer S (2012) Harnessing snap-through instability in soft dielectrics to achieve giant voltage-triggered deformation. Soft Matter 8(2):285–288

Kim BJ, Meng E (2015) Review of polymer MEMS micromachining. J Micromech Microeng 26(1):013001

Kim KH, Yoon HJ, Jeong OC, Yang SS (2005) Fabrication and test of a micro electromagnetic actuator. Sens Actuators A 117(1):8–16

Kofod G, Wirges W, Paajanen M, Bauer S (2007) Energy minimization for self-organized structure formation and actuation. Appl Phys Lett 90(8):081916

Kornbluh RD, Pelrine R, Prahlad H, Wong-Foy A, McCoy B, Kim S, Low T et al (2012) Dielectric elastomers: Stretching the capabilities of energy harvesting. MRS Bull 37(3):246–253

Kwon GH, Park JY, Kim JY, Frisk ML, Beebe DJ, Lee SH (2008) Biomimetic soft multifunctional miniature aquabots. Small 4(12):2148–2153

Lee C-Y, Chen Z-H, Chang H-T, Wen C-Y, Cheng C-H (2009) Design and fabrication of novel micro electromagnetic actuator. Microsyst Technol 15(8):1171–1177

Lee JH, Okamoto S, Matsubara S (2012) Development of multi-fingered prosthetic hand using shape memory alloy type artificial muscle. Comput Technol Appl 3(7)

Lee C, Choi H, Go G, Jeong S, Ko SY, Park J-O, Park S (2014a) Active locomotive intestinal capsule endoscope (ALICE) system: a prospective feasibility study. IEEE/ASME Trans Mechatron 20(5):2067–2074

Lee HS, Phung H, Lee D-H, Kim UK, Nguyen CT, Moon H, Choi HR et al (2014b) Design analysis and fabrication of arrayed tactile display based on dielectric elastomer actuator. Sens Actuators A 205:191–198

Lee C, Kim U, Lee D-H, Nguyen CT, Nguyen DT, Phung H, Choi HR et al (2017) Development of a smart handheld surgical tool with tactile feedback. Intell Serv Robot 10(2):149–158

Lee HT, Kim MS, Lee GY, Kim CS, Ahn SH (2018) Shape memory alloy (SMA)-based microscale actuators with 60% deformation rate and 1.6 kHz actuation speed. Small 14(23):1801023

Li C, Gu X, Xiao X, Lim CM, Ren H (2018) A robotic system with multichannel flexible parallel manipulators for single port access surgery. IEEE Trans Ind Inf 15(3):1678–1687

Li J, Zhou X, Zhao H, Shao M, Hou P, Xu X (2015) Design and experimental performances of a piezoelectric linear actuator by means of lateral motion. Smart Mater Struct 24(6):065007

Liang C, Wang F, Shi B, Huo Z, Zhou K, Tian Y, Zhang D (2018) Design and control of a novel asymmetrical piezoelectric actuated microgripper for micromanipulation. Sens Actuators A 269:227–237

Linnebach P, Rizzello G, Seelecke S (2020) Design and validation of a dielectric elastomer membrane actuator driven pneumatic pump. Smart Mater Struct 29(7):075021

Liu C, Qin H, Mather PT (2007) Review of progress in shape-memory polymers. J Mater Chem 17(16):1543–1558

Liu G, Shen C, Yang Z, Cai X, Zhang H (2010) A disposable piezoelectric micropump with high performance for closed-loop insulin therapy system. Sens Actuators A 163(1):291–296

Liu Y, Hao Z, Yu J, Zhou X, Lee PS, Sun Y, Zeng F et al (2019) A high-performance soft actuator based on a poly (vinylidene fluoride) piezoelectric bimorph. Smart Mater Struct 28(5):055011

Liu Y, Yang Y, Peng Y, Zhong S, Liu N, Pu H (2020) A light soft manipulator with continuously controllable stiffness actuated by a thin McKibben pneumatic artificial muscle. IEEE/ASME Trans Mechatron 25(4):1944–1952

Lu Y, Xie Z, Wang J, Yue H, Wu M, Liu Y (2019) A novel design of a parallel gripper actuated by a large-stroke shape memory alloy actuator. Int J Mech Sci 159:74–80

Lv X, Wei W, Mao X, Chen Y, Yang J, Yang F (2015) A novel MEMS electromagnetic actuator with large displacement. Sens Actuators A 221:22–28

Ma H-K, Luo W-F, Lin J-Y (2015a) Development of a piezoelectric micropump with novel separable design for medical applications. Sens Actuators A 236:57–66

Ma H, Chen R, Hsu Y (2015b) Development of a piezoelectric-driven miniature pump for biomedical applications. Sens Actuators A 234:23–33

Madsen FB, Yu L, Daugaard AE, Hvilsted S, Skov AL (2014) Silicone elastomers with high dielectric permittivity and high dielectric breakdown strength based on dipolar copolymers. Polymer 55(24):6212–6219

Maffli L, Rosset S, Ghilardi M, Carpi F, Shea H (2015) Ultrafast all-polymer electrically tunable silicone lenses. Adv Funct Mater 25(11):1656–1665

Makino E, Mitsuya T, Shibata T (2001) Fabrication of TiNi shape memory micropump. Sens Actuators A 88(3):256–262

McDaid A, Xie S, Aw K (2012) A compliant surgical robotic instrument with integrated IPMC sensing and actuation. Int J Smart Nano Mater 3(3):188–203

Mehrabi H, Aminzahed I (2020) Design and testing of a microgripper with SMA actuator for manipulation of micro components. Microsyst Technol 26(2):531–536

Mehrpouya M, Cheraghi Bidsorkhi H (2016) MEMS applications of NiTi based shape memory alloys: a review. Micro Nanosyst 8(2):79–91

Mirvakili SM, Hunter IW (2018) Artificial muscles: mechanisms, applications, and challenges. Adv Mater 30(6):1704407

Mitchell SK, Wang X, Acome E, Martin T, Ly K, Kellaris N, Keplinger C et al (2019) An easy-to-implement toolkit to create versatile and high-performance HASEL actuators for untethered soft robots. Adv Sci 6(14):1900178

Moglia A, Menciassi A, Schurr MO, Dario P (2007) Wireless capsule endoscopy: from diagnostic devices to multipurpose robotic systems. Biomed Microdevice 9(2):235–243

Mohith S, Karanth PN, Kulkarni SM (2019) Recent trends in mechanical micropumps and their applications: A review. Mechatronics 60:34–55

Mohith S, Karanth N, Kulkarni S (2020) Performance analysis of valveless micropump with disposable chamber actuated through amplified piezo actuator (APA) for biomedical application. Mechatronics 67:102347

Mu T, Liu L, Lan X, Liu Y, Leng J (2018) Shape memory polymers for composites. Compos Sci Technol 160:169–198. https://doi.org/10.1016/j.compscitech.2018.03.018

Munas FR, Melroy G, Abeynayake CB, Chathuranga HL, Amarasinghe R, Kumarage P, Dao DV et al (2018) Development of PZT actuated valveless micropump. Sensors 18(5):1302

Munoz F, Alici G, Li W (2014) A review of drug delivery systems for capsule endoscopy. Adv Drug Delivery Rev 71:77–85

Munasinghe KC, Bowatta BGCT, Abayarathne HYR, Kumararathna N, Maduwantha LKAH, Arachchige NMP, Amarasinghe YWR (2016) New MEMS based micro gripper using SMA for micro level object manipulation and assembling. In: Moratuwa Engineering Research Conference (MERCon), pp 36–41

Na Y-M, Lee H-S, Park J-K (2018) Fabrication and experiment of piezoelectric pump imitating peristalsis. J Mech Sci Technol 32(10):4737–4745

Naclerio ND, Hawkes EW (2020) Simple, low-hysteresis, foldable, fabric pneumatic artificial muscle. IEEE Robot Autom Lett 5(2):3406–3413

Nafea M, Nawabjan A, Ali MSM (2018) A wirelessly-controlled piezoelectric microvalve for regulated drug delivery. Sens Actuators A 279:191–203

Nah S, Zhong Z (2007) A microgripper using piezoelectric actuation for micro-object manipulation. Sens Actuators A 133(1):218–224

Namazu T, Komatsubara M, Nagasawa H, Miki T, Tsurui T, Inoue S (2011) Titanium-nickel shape memory alloy spring actuator for forward-looking active catheter. J Metall

Nguyen CT, Phung H, Hoang PT, Nguyen TD, Jung H, Moon H, Choi HR (2017) A novel bioinspired hexapod robot developed by soft dielectric elastomer actuators. In: IEEE/RSJ International Conference on Intelligent Robots and Systems (IROS), pp 6233–6238

Niiyama R, Sun X, Sung C, An B, Rus D, Kim S (2015) Pouch motors: printable soft actuators integrated with computational design. Soft Robot 2(2):59–70

Nikpourian A, Ghazavi MR, Azizi S (2019) Size-dependent nonlinear behavior of a piezoelectrically actuated capacitive bistable microstructure. Int J Non-Linear Mech 114:49–61

Ohta P, Valle L, King J, Low K, Yi J, Atkeson CG, Park Y-L (2018) Design of a lightweight soft robotic arm using pneumatic artificial muscles and inflatable sleeves. Soft Robot 5(2):204–215

Oxley TJ, Opie NL, John SE, Rind GS, Ronayne SM, Wheeler TL, Lovell TJ et al (2016) Minimally invasive endovascular stent-electrode array for high-fidelity, chronic recordings of cortical neural activity. Nat Biotechnol 34(3):320–327

Paez L, Agarwal G, Paik J (2016) Design and analysis of a soft pneumatic actuator with origami shell reinforcement. Soft Robot 3(3):109–119

Pan P, Wang W, Ru C, Sun Y, Liu X (2017) MEMS-based platforms for mechanical manipulation and characterization of cells. J Micromech Microeng 27(12):123003

Park I-S, Jung K, Kim D, Kim S-M, Kim KJ (2008) Physical principles of ionic polymer–metal composites as electroactive actuators and sensors. MRS Bull 33(3):190–195

Park B, Afsharipour E, Chrusch D, Shafai C, Andersen D, Burley G (2017) Large displacement bi-directional out-of-plane Lorentz actuator array for surface manipulation. J Micromech Microeng 27(8):085005

Park H-B, Kim D-R, Kim H-J, Wang W, Han M-W, Ahn S-H (2020) Design and analysis of artificial muscle robotic elbow joint using shape memory alloy actuator. Int J Precis Eng Manuf 21(2):249–256

Paul SR, Nayak SK, Anis A, Pal K (2016) MEMS-based controlled drug delivery systems: a short review. Polym-Plast Technol Eng 55(9):965–975

Pawinanto RE, Yunas J, Majlis BY, Hamzah AA (2016) Design and fabrication of compact MEMS electromagnetic micro-actuator with planar micro-coil based on PCB. Telkomnika 14(3):856–866

Pečar B, Križaj D, Vrtačnik D, Resnik D, Dolžan T, Možek M (2014) Piezoelectric peristaltic micropump with a single actuator. J Micromech Microeng 24(10):105010

Pei Q, Rosenthal M, Stanford S, Prahlad H, Pelrine R (2004) Multiple-degrees-of-freedom electroelastomer roll actuators. Smart Mater Struct 13(5):N86

Pelrine R, Kornbluh R, Pei Q, Joseph J (2000) High-speed electrically actuated elastomers with strain greater than 100%. Science 287(5454):836–839

Peng J, Chen X (2013) A survey of modeling and control of piezoelectric actuators. Mod Mech Eng 3(01):1

Peng T, Guo Q, Yang J, Xiao J, Wang H, Lou Y, Liang X (2019) A high-flow, self-filling piezoelectric pump driven by hybrid connected multiple chambers with umbrella-shaped valves. Sens Actuators B Chem 301:126961

Perez-Guagnelli E, Jones J, Tokel AH, Herzig N, Jones B, Miyashita S, Damian DD (2020) Characterization, simulation and control of a soft helical pneumatic implantable robot for tissue regeneration. IEEE Trans Med Robot Bionics 2(1):94–103

Pradeep A, Stanley J, Nair BG, Babu TGS (2018) Automated and programmable electromagnetically actuated valves for microfluidic applications. Sensors Actuators A Phys 283:79–86

Pringpromsuk S, Xia H, Ni Q-Q (2020) Multifunctional stimuli-responsive shape memory polyurethane gels for soft actuators. Sens Actuators A 313:112207

Pringpromsuk S, Xia H, Ni Q-Q (2021) Thermal triggering on plasticized shape memory polyurethane actuators and its tubes target to biomedical applications. Sens Actuators A 332:113164

Qi C, Han D, Shinshi T (2021) A MEMS-based electromagnetic membrane actuator utilizing bonded magnets with large displacement. Sens Actuators A 330:112834

Qian J-Y, Hou C-W, Li X-J, Jin Z-J (2020) Actuation mechanism of microvalves: a review. Micromachines 11(2):172

Qin L, Cao J, Tang Y, Zhu J (2018) Soft freestanding planar artificial muscle based on dielectric elastomer actuator. J Appl Mech 85(5):051001

Qiu Y, Zhang E, Plamthottam R, Pei Q (2019) Dielectric elastomer artificial muscle: materials innovations and device explorations. Acc Chem Res 52(2):316–325

Rahbar M, Gray BL (2017) Maximizing deflection in MEMS and microfluidic actuators fabricated in permanently magnetic composite polymers. In: IEEE 17th International Conference on Nanotechnology (IEEE-NANO), pp 466–470

Rahimi S, Sarraf EH, Wong GK, Takahata K (2011) Implantable drug delivery device using frequency-controlled wireless hydrogel microvalves. Biomed Microdevice 13(2):267–277

Ranzani T, Gerboni G, Cianchetti M, Menciassi A (2015) A bioinspired soft manipulator for minimally invasive surgery. Bioinspir Biomim 10(3):035008

Razif MRM, Bavandi M, Nordin INAM, Natarajan E, Yaakob O (2014) Two chambers soft actuator realizing robotic gymnotiform swimmers fin. In: IEEE International Conference on Robotics and Biomimetics (ROBIO 2014), pp 15–20

Rehman T, Faudzi AAM, Dewi DEO, Ali MSM (2017) Design, characterization, and manufacturing of circular bellows pneumatic soft actuator. Int J Adv Manufact Technol 93:4295–4304

Rehman T, Nafea M, Faudzi AA, Saleh T, Ali MSM (2019) PDMS-based dual-channel pneumatic micro-actuator. Smart Mater Struct 28(11):115044

Ren Z, Yuan J, Su X, Xu Y, Bauer R, Mangla S, Shi Y et al (2020). Multilayered microstructures with shape memory effects for vertical deployment. Microsyst Technol 1–8

Rosset S, Shea HR (2013) Flexible and stretchable electrodes for dielectric elastomer actuators. Appl Phys A 110(2):281–307

Rosset S, Shea HR (2016) Small, fast, and tough: Shrinking down integrated elastomer transducers. Appl Phys Rev 3(3):031105

Rosset S, O'Brien BM, Gisby T, Xu D, Shea HR, Anderson IA (2013) Self-sensing dielectric elastomer actuators in closed-loop operation. Smart Mater Struct 22(10):104018

Rothemund P, Kellaris N, Keplinger C (2019) How inhomogeneous zipping increases the force output of Peano-HASEL actuators. Extreme Mech Lett 31:100542

Rothemund P, Kellaris N, Mitchell SK, Acome E, Keplinger C (2021) HASEL artificial muscles for a new generation of lifelike robots—recent progress and future opportunities. Adv Mater 33(19):2003375

Rusli M, Chee PS, Arsat R, Lau KX, Leow PL (2018) Electromagnetic actuation dual-chamber bidirectional flow micropump. Sens Actuators A 282:17–27

Ruzzu A, Bade K, Fahrenberg J, Maas D (1998) Positioning system for catheter tips based on an active microvalve system. J Micromech Microeng 8(2):161

Salim M, Salim D, Chandran D, Aljibori HS, Kherbeet AS (2018) Review of nano piezoelectric devices in biomedicine applications. J Intell Mater Syst Struct 29(10):2105–2121

Sanan S, Lynn PS, Griffith ST (2014) Pneumatic torsional actuators for inflatable robots. J Mech Robot 6(3):031003

Sassa F, Al-Zain Y, Ginoza T, Miyazaki S, Suzuki H (2012) Miniaturized shape memory alloy pumps for stepping microfluidic transport. Sens Actuators B Chem 165(1):157–163

Schmidt-Rohr K, Chen Q (2008) Parallel cylindrical water nanochannels in Nafion fuel-cell membranes. Nat Mater 7(1):75–83

Sénac T, Lelevé A, Moreau R, Novales C, Nouaille L, Pham MT, Vieyres P (2019) A review of pneumatic actuators used for the design of medical simulators and medical tools. Multimodal Technol Interact 3(3):47

Shabalovskaya SA (1996) On the nature of the biocompatibility and on medical applications of NiTi shape memory and superelastic alloys. Bio-Med Mater Eng 6(4):267–289

Shahinpoor M (2003) Mechanoelectrical phenomena in ionic polymers. Math Mech Solids 8(3):281–288

Shahinpoor M, Kim KJ (2001) Ionic polymer-metal composites: I. Fundam Smart Mater Struct 10(4):819

Shahinpoor M, Kim KJ (2004) Ionic polymer–metal composites: IV. Industrial and medical applications. Smart Mater Struct 14(1):197

Sheeparamatti BG, Naik VV (2016) Exploration of micro cantilever based electromagnetic actuator. In: International Conference on Electrical, Electronics, Communication, Computer and Optimization Techniques (ICEECCOT), pp 350–354

Sheima Y, Caspari P, Opris DM (2019) Artificial muscles: dielectric elastomers responsive to low voltages. Macromol Rapid Commun 40(16):e1900205

Shi H, Chen J, Liu G, Xiao W, Dong S (2013) A piezoelectric pseudo-bimorph actuator. Appl Phys Lett 102(24):242904

Shi ZY, Liu D, Wang TM (2014) A shape memory alloy-actuated surgical instrument with compact volume. Int J Med Robot Comput Assist Surg 10(4):474–481

Shintake J, Sonar H, Piskarev E, Paik J, Floreano D (2017) Soft pneumatic gelatin actuator for edible robotics. In: IEEE/RSJ International Conference on Intelligent Robots and Systems (IROS), pp 6221–6226

Shintake J, Cacucciolo V, Floreano D, Shea H (2018a) Soft robotic grippers. Adv Mater 30(29):1707035

Shintake J, Cacucciolo V, Shea H, Floreano D (2018b) Soft biomimetic fish robot made of dielectric elastomer actuators. Soft Rob 5(4):466–474

Singh J, Kumar A, Chelvane JA (2019) Stress compensated MEMS magnetic actuator based on magnetostrictive Fe65Co35 thin films. Sens Actuators A 294:54–60

Solano-Arana S, Klug F, Mößinger H, Förster-Zügel F, Schlaak HF (2018) A novel application of dielectric stack actuators: a pumping micromixer. Smart Mater Struct 27(7):074008

Sonar HA, Gerratt AP, Lacour SP, Paik J (2020) Closed-loop haptic feedback control using a self-sensing soft pneumatic actuator skin. Soft robot 7(1):22–29

Spagna JC, Peattie AM (2012) Terrestrial locomotion in arachnids. J Insect Physiol 58(5):599–606

Srinivasa Rao K, Hamza M, Ashok Kumar P, Girija Sravani K (2020) Design and optimization of MEMS based piezoelectric actuator for drug delivery systems. Microsyst Technol 26(5):1671–1679

Sun Z, Hao L, Chen W, Li Z, Liu L (2013) A novel discrete adaptive sliding-mode-like control method for ionic polymer–metal composite manipulators. Smart Mater Struct 22:095027

Sun N, Liang D, Wu Y, Chen Y, Qin Y, Fang Y (2019) Adaptive control for pneumatic artificial muscle systems with parametric uncertainties and unidirectional input constraints. IEEE Trans Industr Inf 16(2):969–979

Sun L, Gao X, Wu D, Guo Q (2021) Advances in physiologically relevant actuation of shape memory polymers for biomedical applications. Polym Rev 61(2):280–318

Surakusumah RF, Dewi DEO, Supriyanto E (2014) Development of a half sphere bending soft actuator for flexible bronchoscope

movement. In: IEEE International Symposium on Robotics and Manufacturing Automation (ROMA), pp 120–125

Suzumori K (1996) Elastic materials producing compliant robots. Robot Auton Syst 18(1–2):135–140

Suzumori K, Endo S, Kanda T, Kato N, Suzuki H (2007) A bending pneumatic rubber actuator realizing soft-bodied manta swimming robot. In: Proceedings IEEE International Conference on Robotics and Automation, pp 4975–4980

Takizawa T, Kanno T, Miyazaki R, Tadano K, Kawashima K (2018) Grasping force estimation in robotic forceps using a soft pneumatic actuator with a built-in sensor. Sens Actuators A: Phys 271:124–130

Tang Y, Qin L, Li X, Chew CM, Zhu J (2017) A frog-inspired swimming robot based on dielectric elastomer actuators. In: IEEE/RSJ International Conference on Intelligent Robots and Systems (IROS), pp 2403–2408

Taniguchi H (2013) Flexible artificial muscle actuator using coiled shape memory alloy wires. APCBEE Proc 7:54–59

Tetteh EA, Boatemaa MA, Martinson EO (2014) A review of various actuation methods in micropumps for drug delivery appliactions. In: 11th International Conference on Electronics, Computer and Computation (ICECCO), pp 1–4

Thierry B, Merhi Y, Bilodeau L, Trepanier C, Tabrizian M (2002) Nitinol versus stainless steel stents: acute thrombogenicity study in an ex vivo porcine model. Biomaterials 23(14):2997–3005

Toennies JL, Tortora G, Simi M, Valdastri P, Webster R (2010) Swallowable medical devices for diagnosis and surgery: the state of the art. Proc Inst Mech Eng C J Mech Eng Sci 224(7):1397–1414

Ullrich F, Dheman KS, Schuerle S, Nelson BJ (2015) Magnetically actuated and guided milli-gripper for medical applications. In: IEEE International Conference on Robotics and Automation (ICRA), pp 1751–1756

Vaicekauskaite J, Mazurek P, Vudayagiri S, Skov AL (2020) Mapping the mechanical and electrical properties of commercial silicone elastomer formulations for stretchable transducers. J Mater Chem C 8(4):1273–1279

Vartholomeos P, Qin L, Dupont PE (2011) MRI-powered actuators for robotic interventions. In: IEEE/RSJ International Conference on Intelligent Robots and Systems, pp 4508–4515

Wache H, Tartakowska D, Hentrich A, Wagner M (2003) Development of a polymer stent with shape memory effect as a drug delivery system. J Mater Sci Mater Med 14(2):109–112

Wakimoto S, Kumagai I, & Suzumori K (2009). Development of large intestine endoscope changing its stiffness. In: IEEE International Conference on Robotics and Biomimetics (ROBIO), pp 2320–2325

Wakimoto S, Ogura K, Suzumori K, Nishioka Y (2009) Miniature soft hand with curling rubber pneumatic actuators. In: IEEE International Conference on Robotics and Automation, pp 556–561

Wang L, Chen W, Liu J, Deng J, Liu Y (2019) A review of recent studies on non-resonant piezoelectric actuators. Mech Syst Signal Process 133:106254

Wang Q-M, Cross LE (1998) Performance analysis of piezoelectric cantilever bending actuators. Ferroelectrics 215(1):187–213

Wang H, El Wahed AK (2020) Development of a novel latching-type electromagnetic actuator for applications in minimally invasive surgery. In Actuators 9(2):41

Wang X, Mitchell SK, Rumley EH, Rothemund P, Keplinger C (2020) High-strain peano-HASEL actuators. Adv Func Mater 30(7):1908821

Wang Y, Zhi C, Tang B, Yang K, Xie J, Xu W, Wang X et al (2021)

A micro electromagnetic actuator with high force density. Sens Actuators A Phys 112771

Wu W, Zhang S, Wu Z, Qin S, Li F, Song T, Zhang L et al (2021) On the understanding of dielectric elastomer and its application for all-soft artificial heart. Sci Bull 66(10):981–990

Xavier MS, Tawk CD, Yong YK, Fleming AJ (2021) 3D-printed omnidirectional soft pneumatic actuators: Design, modeling and characterization. Sens Actuators A 332:113199

Yahara S, Wakimoto S, Kanda T, Matsushita K (2019) McKibben artificial muscle realizing variable contraction characteristics using helical shape-memory polymer fibers. Sens Actuators A 295:637–642

Yanatori H, Tsuji K, Abe K, Iwasaki K, Mineta T (2019) Fabrication and characterization of an arrayed shape memory alloy thick film actuator device for planar tactile displays. IEEJ Trans Sens Micromach 139(1):15–20

Yang S, Xu Q (2017) A review on actuation and sensing techniques for MEMS-based microgrippers. J Micro-Bio Robot 13(1):1–14

Yang Y, Chen Y, Wei Y, Li Y (2016) Novel design and three-dimensional printing of variable stiffness robotic grippers. J Mech Robot 8(6):061010

Yang HD, Greczek BT, Asbeck AT (2019) Modeling and analysis of a high-displacement pneumatic artificial muscle with integrated sensing. Front Robot AI 5:136

Younis MI (2011) MEMS linear and nonlinear statics and dynamics, vol 20. Springer Science & Business Media

Yuan X, Liu D, Gong M (2014) Design and research on a shape memory alloy-actuated single-port laparoscopic surgical robot. In: IEEE International Conference on Mechatronics and Automation, pp 1654–1658

Yunas J, Mulyanti B, Hamidah I, Mohd Said M, Pawinanto RE, Wan Ali WAF, Yeop Majlis B (2020) Polymer-based MEMS electromagnetic actuator for biomedical application: A review. Polymers 12(5):1184

Zainal MA, Ahmad A, Mohamed Ali MS (2017) Frequency-controlled wireless shape memory polymer microactuator for drug delivery application. Biomed Microdevices 19:1–10

Zainal MA, Ali MSM (2016) Wireless shape memory polymer microactuator for implantable drug delivery aplication. In: IEEE EMBS Conference on Biomedical Engineering and Sciences (IECBES), pp 76–79

Zainal MA, Sahlan S, Ali MSM (2015) Micromachined shape-memory-alloy microactuators and their application in biomedical devices. Micromachines 6(7):879–901

Ze Q, Kuang X, Wu S, Wong J, Montgomery SM, Zhang R, Zhao R et al (2020) Magnetic shape memory polymers with integrated multifunctional shape manipulation. Adv Mater 32(4):1906657

Zhang Z, Kan J, Wang S, Wang H, Wen J, Ma Z (2013) Flow rate self-sensing of a pump with double piezoelectric actuators. Mech Syst Signal Process 41(1–2):639–648

Zhang Z, Kan JW, Wang S, Wang H, Ma J, Jiang Y (2016) Development of a self-sensing piezoelectric pump with a bimorph transducer. J Intell Mater Syst Struct 27(5):581–591

Zhang Y, Peng Y, Sun Z, Yu H (2018) A novel stick–slip piezoelectric actuator based on a triangular compliant driving mechanism. IEEE Trans Ind Electron 66(7):5374–5382

Zhang B, Hu C, Yang P, Liao Z, Liao H (2019a) Design and modularization of multi-DoF soft robotic actuators. IEEE Robot Autom Lett 4(3):2645–2652

Zhang Y, Ellingford C, Zhang R, Roscow J, Hopkins M, Keogh P, Wan C et al (2019b) Electrical and mechanical self-healing in high-performance dielectric elastomer actuator materials. Adv Func Mater 29(15):1808431

Zhang YF, Zhang N, Hingorani H, Ding N, Wang D, Yuan C, Ge Q et al (2019c) Fast-response, stiffness-tunable soft actuator by hybrid multimaterial 3D printing. Adv Func Mater 29(15):1806698

Zhang B, Huang Y, He L, Xu Q, Cheng G (2020) Research on double-outlet valveless piezoelectric pump with fluid guiding body. Sens Actuators A 302:111785

Zhao X, Suo Z (2010) Theory of dielectric elastomers capable of giant deformation of actuation. Phys Rev Lett 104(17):178302

Zhao D, He L-P, Li W, Huang Y, Cheng G-M (2019) Experimental analysis of a valve-less piezoelectric micropump with crescent-shaped structure. J Micromech Microeng 29(10):105004

Zhou Y, Amirouche F (2011) An electromagnetically-actuated all-PDMS valveless micropump for drug delivery. Micromachines 2(3):345–355